

# Towards formalization of the soliton counting technique for the Khovanov–Rozansky invariants in the deformed $\mathcal{R}$ -matrix approach

A. Anokhina\*

## Abstract

We consider recently developed Cohomological Field Theory (CohFT) soliton counting diagram technique for Khovanov (Kh) and Khovanov–Rozansky (KhR) invariants [1, 2]. Although the expectation to obtain a new way for computing the invariants has not yet come true, we demonstrate that soliton counting technique can be totally formalized at an intermediate stage, at least in particular cases. We present the corresponding algorithm, based on the approach involving deformed  $\mathcal{R}$ -matrix and minimal positive division, developed previously in [3]. We start from a detailed review of the minimal positive division approach, comparing it with other methods, including the rigorous mathematical treatment [4]. Pieces of data obtained within our approach are presented in the Appendices.

## Contents

<b>1</b>	<b>Introduction</b>	<b>2</b>
1.1	Different approaches to KhR invariants . . . . .	4
1.2	Conjectures and expectations . . . . .	4
<b>2</b>	<b>A sketch of the general construction</b>	<b>4</b>
2.1	The necessary notions of knot and representation theory . . . . .	4
2.2	Explicit expression for knot invariants . . . . .	8
2.3	Resolution hypercube . . . . .	8
2.4	Vector spaces at the hypercube vertices . . . . .	11
2.5	Spaces at the vertices as graded spaces . . . . .	12
2.6	From the resolution hypercube to the complex . . . . .	13
2.7	Graded basis in the homologies . . . . .	14
2.8	The geometric meaning of the positive integer decomposition . . . . .	14
<b>3</b>	<b>Minimal positive division instead of computing the homology</b>	<b>15</b>
3.1	General definitions . . . . .	15
3.1.1	Complex, homologies and decomposition of the generating functions. . . . .	15
3.1.2	Integer and polynomial division. . . . .	16
3.1.3	Division as homology computation . . . . .	17
3.2	“Ambiguous” and “unambiguous” minimal remainders . . . . .	17
3.3	Properties of maps as “selection rules” for the “minimal remainder” . . . . .	18
3.3.1	Ranks of the differentials . . . . .	18
3.3.2	Particular values of matrix elements . . . . .	19
3.4	“Multilevel” division as a way to fix ambiguities . . . . .	20
<b>4</b>	<b>Lie algebra structure in the complex and its breaking</b>	<b>20</b>
4.1	The idea . . . . .	21
4.2	Spaces in the resolution hypercube as representation spaces . . . . .	21
4.3	Are the homology spaces representation spaces? . . . . .	22
4.3.1	A toy example . . . . .	23
4.3.2	Relation to the real case . . . . .	23

---

\*ITEP, Moscow, Russia; anokhina@itep.ru

<b>5</b>	<b>Differential expansion and evolution method</b>	<b>24</b>
5.0.1	The sketch of the methods . . . . .	24
5.0.2	The interplay with the positive division method . . . . .	24
5.0.3	The interplay with the group theory viewpoint . . . . .	25
<b>6</b>	<b>Minimal positive division approach and CohFT calculus</b>	<b>25</b>
6.1	Preliminary comments . . . . .	25
6.1.1	CohFT diagram technique . . . . .	25
6.1.2	Selection rule for CohFT matrix elements . . . . .	25
6.1.3	Types of CohFT matrix elements and multilevel division . . . . .	26
6.1.4	Our program . . . . .	26
6.2	Division algorithm for a generic two strand knot . . . . .	26
6.2.1	The CohFT calculus in the two-strand case . . . . .	26
6.2.2	Khovanov ( $N = 2$ ) case . . . . .	27
6.2.3	KhR for generic $N$ . . . . .	28
6.2.4	Primary polynomials as “deformed” HOMFLY polynomials . . . . .	28
6.2.5	Comparing the $N = 2$ and $N > 2$ cases . . . . .	29
6.2.6	The primary polynomial as the generating function for the soliton diagrams . . . . .	30
6.2.7	Example: torus knot $T^{2,5}$ . . . . .	32
6.3	The first-level division for particular three-strand knots . . . . .	32
6.3.1	A draft of the three-strand reduction procedure . . . . .	32
6.3.2	Explicit formulas for the three-strand (deformed) $\mathcal{R}$ -matrices . . . . .	34
6.4	The generating function for the three-strand soliton diagrams . . . . .	35
6.4.1	Guide to the experimental data . . . . .	35
<b>7</b>	<b>Further directions</b>	<b>35</b>
<b>A</b>	<b>Basic properties of the special point operators</b>	<b>38</b>
A.1	General constraints on the special point operators . . . . .	38
A.1.1	Continuous space transformations and transformations of the knot diagram. . . . .	38
A.1.2	Topological invariance constraints on the crossing and turning point operators. . . . .	39
A.2	Constraints on the $\mathcal{R}$ -matrices . . . . .	39
A.3	Relations between the $\mathcal{R}$ and $\mathcal{Q}$ -matrices . . . . .	39
A.4	Properties of the particular solution . . . . .	40
A.5	Inverting of all crossings and mirror symmetry of the knot invariants . . . . .	41
<b>B</b>	<b>The “graded” basis respected by the differentials</b>	<b>41</b>
<b>C</b>	<b>Morphisms of the representation spaces. A more involved example</b>	<b>42</b>
<b>D</b>	<b>List of braids providing the unique level I reminders</b>	<b>43</b>
<b>E</b>	<b>Examples of the unique minimal remainders related to the CohFT diagrams in the case of three strands</b>	<b>44</b>
E.1	The doubly twisted diagram of the unknot . . . . .	44
E.2	The trefoil knot in different three strand presentations . . . . .	45
E.3	The “thick” knot $8_{19}$ (torus $T[3, 4]$ ) . . . . .	50

## 1 Introduction

Cohomological knot invariants are rather young by knot theory standards. Khovanov invariants (denoted Kh below) [5] were proposed less two decades ago and their Khovanov–Rozanski (KhR) version [4] was introduced less than a decade ago. Both approaches associate a function (precisely, a polynomial) to a knot (or a link),

Table 1: Constructively defined knot invariants

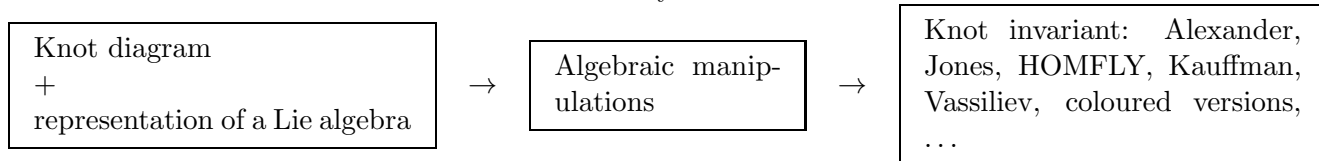
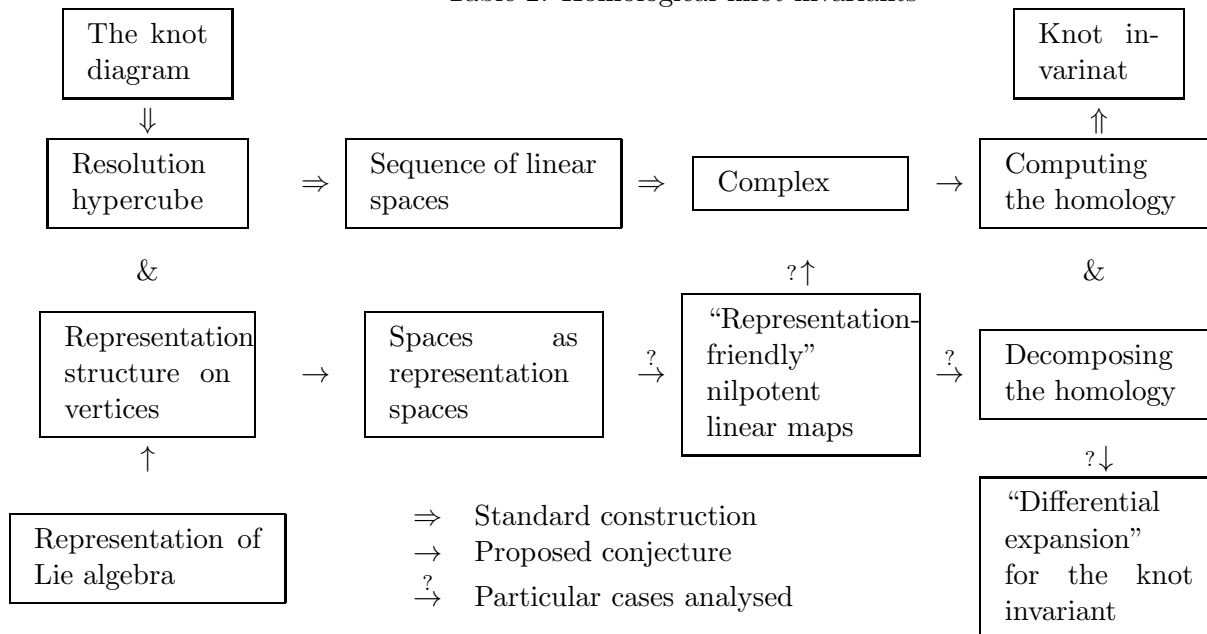


Table 2: Homological knot invariants



so that this function is invariant under arbitrary continuous space transformations. They belong to the wide and well-studied class of polynomial knot invariants [6, 7, 8], although drastically differing from the other ones in their properties. Differences between various knot invariants are illustrated in Tables 1 and 2.

The first and key special point of Khovanov, KhR and other invariants of the same kind [9] is a separate structure associated with a knot, called *knot homology*. The knot polynomial is a generating function for the basis vectors in homologies of a certain complex (and, even worse, in the KhR case the complex of other complexes). This sort of definition, which is multi-level and at many points implicit, causes severe obstacles both for general analysis and for explicit computations. Searches for an alternative approach are naturally quite popular (see, e.g., the references in Table 3).

A closely related quantity is the *superpolynomial* of the knot [10], which remains among the most obscure issues of the knot theory. The superpolynomials are often studied together with the KhR invariants, the connection being two-fold. On the one hand, the superpolynomial is by its only strict (yet not very practical) definition an analytic continuation of the KhR polynomial (similarly to the HOMFLY invariant, which is an analytic continuation of the discrete set of polynomials generalising Jones polynomial<sup>1</sup>. On the other hand, alternative approaches developed for superpolynomials, although being neither general nor mathematically strict in the most cases, proved themselves highly useful both for computations and investigation of general properties of the theory. Hence, the interference of these two subjects may shed light on both super- and KhR polynomials.

A new inspiration in the subject comes from the recently proposed *cohomological field theory* [14], (“CohFT” henceforth) associated with Khovanov and KhR invariants in the same way as Chern-Simons theory is associated with Jones and HOMFLY invariants [15, 16, 17].

In the context of the recent progress of various approaches to the KhR invariants we wish to recall our

<sup>1</sup>However, the naively performed analytical continuation, working well in the HOMFLY case, runs into certain problems in the KhR case [11, 12, 3, 13], see sec. 6.2.5, 7).

own research [3] and compare it with rigorous mathematical treatment, as well as with alternative methods, including the newly proposed CohFT approach.

Various issues concerned here, are summarized and supplied with bibliographic references in Table 3. The rightmost column of the table reflects the structure of the present text.

## 1.1 Different approaches to KhR invariants

## 1.2 Conjectures and expectations

All the viewpoints on the KhR invariants (or superpolynomials) differing from the original one generally aim, speaking most strictly and naively, to obtain the desired invariants just by performing some algebraic manipulations, i.e., to pass by the construction of the complex and the computation of the homologies. In other words, one tries to invent a treatment more in the spirit of the standard knot invariant computations [6].

Because the KhR formalism applies to a complex of complexes, the expectation for its simplification lies on two levels,

1. **The weak expectation** : to find an explicit representation for the spaces and maps in the KhR complex.

In sec. 2 we suggest a way to do this relying on the  $\mathcal{R}$ -matrix formalism (sec. 4 contains some further details). The same method was in fact implicitly used in [3].

2. **The strong expectation** : to skip computing the homologies.

This is the main idea of the minimal positive division technique, developed in [3] which we present in sec. 3 in its abstract form. In 6 we attempt to combine it with the CohFT formalism from [2].

## 2 A sketch of the general construction

### 2.1 The necessary notions of knot and representation theory

Here we briefly review the necessary notions of the knot theory. Details can be found in any knot theory textbook, e.g., in [6].

**Oriented knot in  $\mathbb{R}_3$ .** A knot  $\mathcal{K}$  is by definition an embedding of the oriented circle (e.g., a counterclockwise direction is selected) in the three-dimensional flat space

$$\mathcal{K} : S_1 \hookrightarrow \mathbb{R}_3, \tag{2.1}$$

considered up to continuous transformations of the space  $\mathbb{R}_3$ .

**Diagram of the oriented knot.** The knot can be represented by a knot diagram  $\mathcal{D}$ , which is a planar projection

$$\mathcal{D} : \mathcal{K} \rightarrow \mathbb{R}_2 \tag{2.2}$$

that distinguishes over- and undercrossings of the segments (see example in Fig.1). The selected direction on the knot is preserved on the knot diagram.

As a result,  $\mathcal{D}$  is a planar oriented graph with four-valent vertices (self-crossings), each one having type

 or  up to continuous planar continuous transformations.

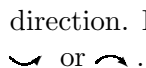



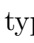





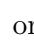
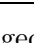
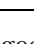
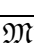
**Extrema on the knot diagram.** In addition, select a direction in the projection plane. Then the special points of the knot projection include, apart from the crossings, the turning points with respect to the direction. Each of the turning-points is treated as a two-valent vertex on the knot diagram, of type  or .

Table 3: Summary of the discussed approaches, with bibliographic and internal references

Khovanov polynomial			$N = 2$
Introduced in	[5]		
Computational technique developed in	[18]		
Table of results, together with computer code	[7]	Presented for all prime knots (up to 11 crossings) and links (up to 11 crossings); in principle, computed for any knots	
Reviewed, e.g., in	[19, 20], [21, 9]		
Khovanov-Rozansky polynomial			$N \in \mathbb{Z}_+$
The definition introduced in	[4]		
Applied to explicit computations in	[11]	“Thin” knots up to 9 crossings	
	[22]	Knots and links up to 6 crossings, mostly for particular vales of $N$	
The approach reviewed, e.g., in	[21, 9]		
Attempts of modification			
Tensor-like formalism	[23]	Simplest examples, 2-strand torus knots, twist knots	
$\mathcal{R}$ -matrix bases formalism	[3]	2 and 3-strand torus knots, 3- and 4-strand knots and links up to 6 crossings, two-component links from two antiparallel strands	ssec. 2, 4
Positive division technique	[3]		ssec. 2.8, 3, 6
CoHFT approach	[14, 1, 2]		sec. 6
Superpolynomial			$0 < N_0 \leq N \in \mathbb{C}$
Introduced in	[10]		
Elvolution method	[24], [25], [26]		sec. 5
Differential expansion	[12], [25], [27], [28], [29]		sec. 5
Finite $N$ problem	[11], [12], [3], [13]		ssec. 6.2.5, 7
coloured generalizations	[30], [24], [25], [27], [28], [31], [9],[32]		sec. 7

Table 4: Sketch of the hypercube calculus for knot invariants

Resolution hypercube $\Sigma$	Complex $\mathcal{V}_0 \xrightarrow{\hat{d}_1} \mathcal{V}_1 \xrightarrow{\hat{d}_2} \dots \xrightarrow{\hat{d}_n} \mathcal{V}_n$		
Vertex $*$	Colouring (resolution) $*$ of the diagram $\mathcal{D}$ of the knot $\mathcal{K}$ , <ul style="list-style-type: none"> <li>• <math>n = \nu_* + \bar{\nu}_*</math> four-valent vertices, <math>\nu_*</math> of  type, <math>\bar{\nu}_*</math> of  type;</li> <li>• <math>2m</math> turning points, <math>m</math> of type  or ,</li> <li><math>m</math> of type  or .</li> </ul>	Operator ${}^*\bar{\mathcal{Z}} \equiv q^{\hat{\Delta}}$ (2.7, 2.13, 2.16) Representation space $\mathcal{V}^* \subset V^{om} = \text{Im } {}^*\bar{\mathcal{Z}}$	sec. 2.1 sec. 2.4 ssec. 2.4, 2.5, 4
Edge $i$		Representation space $V_i$	sec. 2.1
A crossing/ four-valent vertex $\langle k, l i, j \rangle$		Operator $V_i \otimes V_j \mapsto V_k \otimes V_l$	sec. 2
Turning point/ two-valent vertex $\langle \bar{i} i \rangle$		Operator $V_{\bar{i}} \mapsto V_i$	sec. 2.4
 vertex		Identity operator $\text{Id} \otimes \text{Id}$	sec. 2.4
 vertex		“Double” projector $[2]_q \Pi^{\wedge}$ (2.8)	sec. 2.4
Ignored turning point, of type  or 		Identity operator $\text{Id}$	sec. 2.4
Acknowledged turning point, of type 		Operator ${}^*\check{\mathcal{Q}}$ (2.7)	ssec. 2.2, 2.4
Acknowledged turning point, of type 		Operator ${}^*\hat{\mathcal{Q}}$ (2.7)	ssec. 2.2, 2.4
Directed edge $* \rightarrow *'$ , $\nu_* = \nu_{*'} + 1, \bar{\nu}_* = \bar{\nu}_{*'} - 1$		Morphism $\mathfrak{M}_{*'}^* : \mathcal{V}^* \rightarrow \mathcal{V}^{*'}$ , commuting with the grading operator, $\mathfrak{M}_{*'}^* \hat{\Delta} = \hat{\Delta} \mathfrak{M}_{*'}^*$	sec. 2.6 sec. 2.5
Hyperplane $\Xi_k = \bigcup_{\bar{\nu}_*=k}^*$		Representation space $\bigoplus_{\bar{\nu}_*=k}^* \mathcal{V}^*$	ssec. 2.6
Two subsequent hyperplanes, $(\Xi_k, \Xi_{k+1})$		Differential $\hat{d}_k = \bigoplus_{\nu_{*'}=k+1}^{\nu_*=k} \mathfrak{M}_{*'}^*$ , satisfying the nilpotency condition $\hat{d}_{k+1} \hat{d}_k = 0$	sec. 2.6

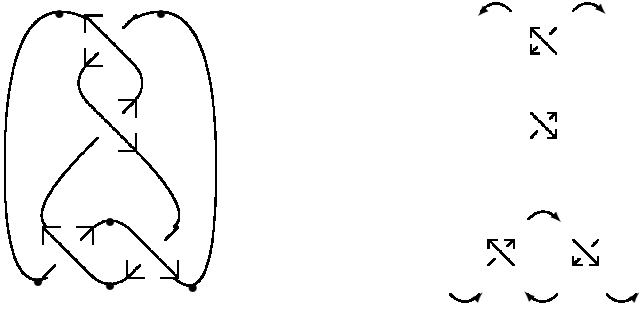


Figure 1: Diagram of the figure-eight knot and the types of the crossings and turning points.

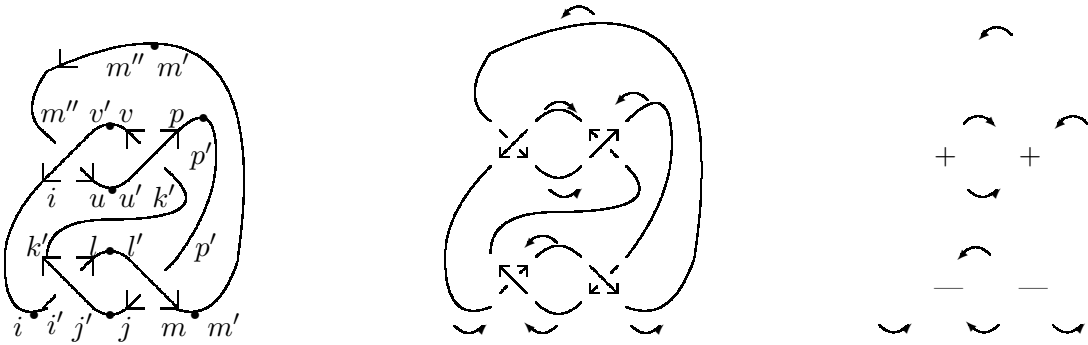


Figure 2: Diagram that represents the same knot  $4_1$  as Fig.1 and contains only two kinds of crossings.

**Representation space on the knot.** The knot is associated with a representation space  $V$  of a Lie algebra  $\mathfrak{g}$ ,

$$\mathcal{K} \rightarrow Y \in \text{rep } \mathfrak{g} \tag{2.3}$$

i.e., one can imagine the linear space  $V$  suspended over each point of the knot. Then one can associate each edge on the knot diagram with the space  $V$ .

**Tensor representation for knot invariants.** As a result, a two-valent vertex (a turning point) of the knot diagram can be related to a linear operator  $Q : V \rightarrow V$ , and a four-valent vertex (a crossing) can be related to a linear operator  $\mathcal{R} : V \otimes V \rightarrow V \otimes V$ .

**The knot diagram as a diagram of the tensor contraction.** The entire diagram  $\mathcal{D}$  represents then the tensor contraction of these operators. To calculate this contraction explicitly, one should

1. Associate to each edge of  $D$  an integer valued label (the number of the basis vector in the space  $V$ ).
2. Multiply the components of  $\mathcal{R}$  and  $Q$  corresponding to all the vertices.
3. Take the sum over all values of the labels (the summation sign is usually omitted in the formulas).

For some specially chosen operators  $\mathcal{R}$  and  $Q$ , the tensor contraction related to the knot diagram turns out to be a topological invariant. Discussing the corresponding constraints (briefly summarised in App. A) on the operators and their general solutions is beyond the scope of our survey. We just write down and use below all the needed explicit expressions.

## 2.2 Explicit expression for knot invariants

Here we present the key points of the  $\mathcal{R}$ -matrix approach to knot invariants (proposed in [33, 34]; see, e.g. textbook [6], or either of the papers [35, 36, 37] for a detailed review).

**Tensor contraction from knot diagram.** The knot diagram must be drawn so that

- both arrows in each crossing have the projections on the preferred direction of the same sign.

In particular, the crossings never coincide with the turning points. One can bring any knot diagram to the required form with the help of continuous planar transformations [6], e.g. the knot represented by the diagram in Fig. 1 is represented by the diagram in fig. 2 as well.

Then, the desired knot invariant is given by the expression<sup>2</sup>

$$\mathcal{H} = \prod_{\substack{\curvearrowright \\ j \ i}} \overset{*}{\mathcal{Q}}_j^i \prod_{\substack{\curvearrowleft \\ j \ i}} \overset{*}{\mathcal{Q}}_j^i \prod_{\substack{\curvearrowright \\ i \ j}} \overset{*}{\mathcal{Q}}_j^i \prod_{\substack{\curvearrowleft \\ i \ j}} \overset{*}{\mathcal{Q}}_j^i \prod_{\substack{l \nearrow k \\ i \ j}} \overset{+}{\mathcal{R}}_{kl}^{ij} \prod_{\substack{k \searrow l \\ j' \ i}} \overset{-}{\mathcal{R}}_{kl}^{ij}. \quad (2.4)$$

E.g., knot diagram in Fig. 2 corresponds to the contraction

$$H^{(\text{fig. 2})} = \overset{-}{\mathcal{R}}_{k'l}^{j'i'} \overset{-}{\mathcal{R}}_{mj}^{l'p'+} \overset{+}{\mathcal{R}}_{iu}^{v'm''+} \overset{+}{\mathcal{R}}_{pv}^{u'k'} \overset{*}{\mathcal{Q}}_{i'}^i \overset{*}{\mathcal{Q}}_{j'}^j \overset{*}{\mathcal{Q}}_{m'}^m \overset{*}{\mathcal{Q}}_{l'}^l \overset{*}{\mathcal{Q}}_u^{u'} \overset{*}{\mathcal{Q}}_v^{v'} \overset{*}{\mathcal{Q}}_{p'}^p \overset{*}{\mathcal{Q}}_{m''}^{m'}. \quad (2.5)$$

**Particular solution for crossing and turning point operators.** Here we consider particular series of solutions for the crossing and turning point operators. Namely, the solution labelled by a positive integer  $N$  corresponds to the Lie group  $\mathfrak{g} = su_N$ ,  $V$  being the space of the fundamental representation<sup>3</sup>, and (in some specially chosen basis) all the non-zero components of the operators have the explicit form<sup>4</sup>

$$\left\{ \begin{array}{l} \overset{+}{\mathcal{R}}_{ii}^{ii} = q, \quad 1 \leq i \leq 1, \\ \overset{+}{\mathcal{R}}_{ji}^{ij} = -1, \quad 1 \leq i \neq j \leq N, \\ \overset{+}{\mathcal{R}}_{ij}^{ij} = q - q^{-1}, \quad 1 \leq i < j \leq N, \end{array} \right\} \left\{ \begin{array}{l} \overset{-}{\mathcal{R}}_{ii}^{ii} = q^{-1}, \quad 1 \leq i \leq 1, \\ \overset{-}{\mathcal{R}}_{ji}^{ij} = -1, \quad 1 \leq i \neq j \leq N, \\ \overset{-}{\mathcal{R}}_{ij}^{ij} = q^{-1} - q, \quad 1 \leq i < j \leq N, \end{array} \right. \quad (2.6)$$

and

$$\overset{*}{\mathcal{Q}}_i^i = q^{N-2i+1}, \quad \overset{*}{\mathcal{Q}}_i^i = q^{2i-1-N}, \quad \overset{*}{\mathcal{Q}}_i^i = 1, \quad \overset{*}{\mathcal{Q}}_i^i = 1, \quad (2.7)$$

$$1 \leq i \leq N.$$

Note that  $\overset{*}{\mathcal{Q}}_j^i = \overset{*}{\mathcal{Q}}_j^i = \delta_j^i$ , hence all the corresponding turning points can just be ignored in (2.4), and we do so henceforth.

## 2.3 Resolution hypercube

Now we turn to the first notion which is used both in Khovanov [5] and KhR [4] constructions, as well as in the alternative approaches under development [23, 3].

<sup>2</sup>We assume the summation over repeated indices.

<sup>3</sup>The solution for any representation of a general Lie group is explicitly written down and discussed, e.g. in [6, 35, 38].

<sup>4</sup>We have already fixed an ambiguity in the definition of the  $\mathcal{Q}$  operators (see App. A). Note that many sources, including [6, 35] fix it differently.



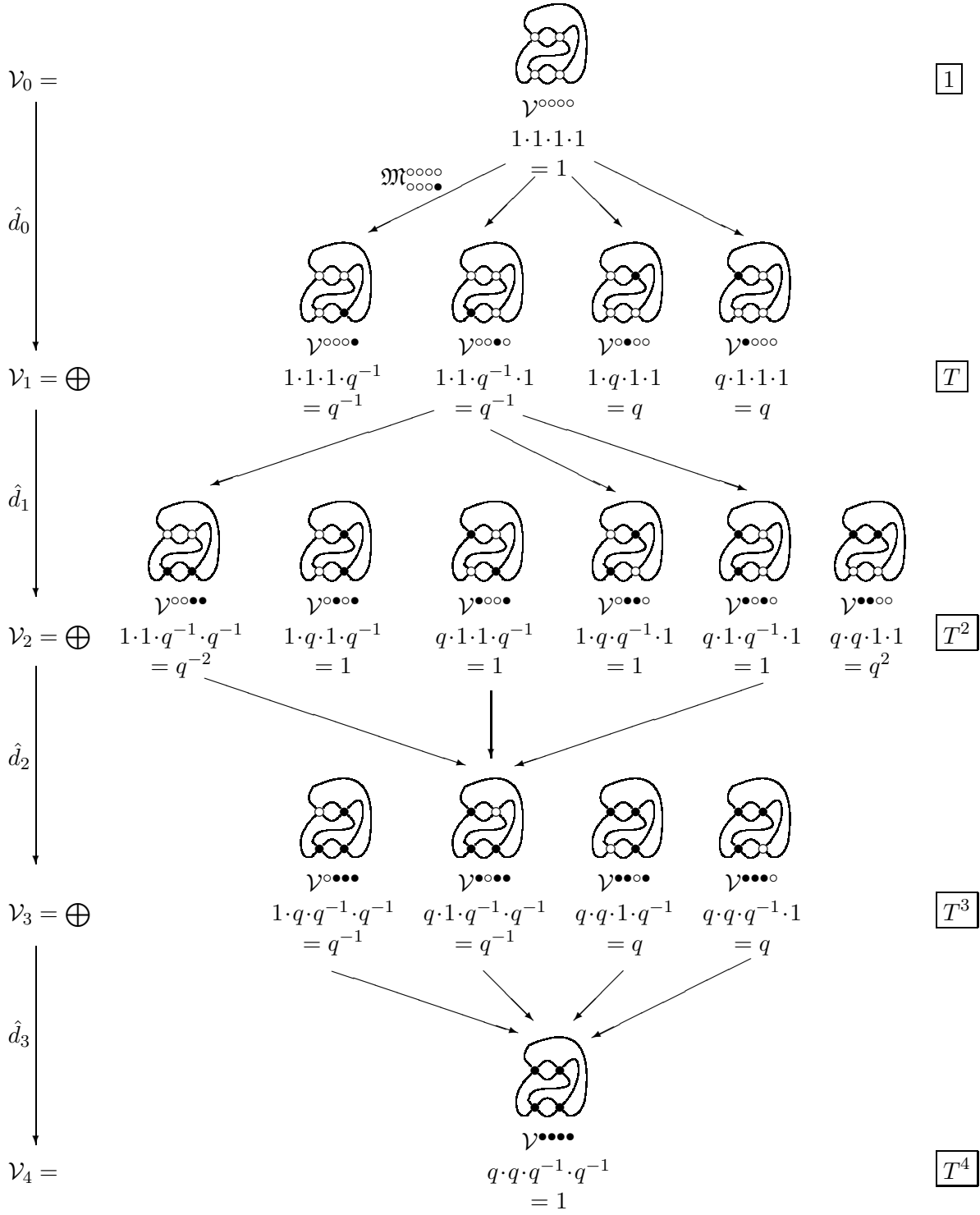


Figure 3: The resolution hypercube for the figure-eight knot (Fig. 2).

**Decomposition for crossing operators.** The operators (2.6) can be identically rewritten as linear combinations of the identity operator and a projector (an operator  $\Pi^\wedge$  such that  $\Pi^\wedge \Pi^\wedge = \Pi^\wedge$ ), namely,

$$\begin{aligned} {}^+\mathcal{R} &= q \circ \mathcal{R} - \bullet \mathcal{R} = q \text{Id} \otimes \text{Id} - [2]_q \Pi^\wedge, \\ {}^-\mathcal{R} &= q^{-1} \circ \mathcal{R} - \bullet \mathcal{R} = q^{-1} \text{Id} \otimes \text{Id} - [2]_q \Pi^\wedge. \end{aligned} \quad (2.8)$$

Formulas (2.8) do not follow from the general group theoretical and topological constraints. They are the special properties of the simplest solution to the constraints, which satisfies characteristic equations (A.9) (see App. A.4).

**Hypercube representation for the knot invariant.** If one substitutes the decomposition (2.8) of the crossing operators in (2.4) and expands the product, the terms of the expansion are enumerated by various *colourings*  $* \in \{\circ, \bullet\}^n$  of the knot diagram, i.e., by the partitions of the  $\circ$  and  $\bullet$  signs (associated with two summands in (2.8)) over the  $n$  crossings.

One can treat the types of crossings as the coordinates,  $\circ = 0$ ,  $\bullet = 1$ . The expansion term associated to the colouring  $*$  thus corresponds to the point of  $n$ -dimensional space with coordinates  $*(\circ = 0, \bullet = 1)$ , so that all the  $2^n$  points form an  $n$ -dimensional hypercube. In turn, an edge (assumed to be directed) of the hypercube connects a pair of colourings related by a flip  $\circ \rightarrow \bullet$ . A vertex  $* \in \text{perm}\{\underbrace{\circ \dots \circ}_{\nu_*}, \underbrace{\bullet \dots \bullet}_{\bar{\nu}_*}\}$  is then connected by  $\nu_*$  incoming and  $\bar{\nu}_* = n - \nu_*$  outgoing arrows to the total of  $n$  vertices from the sets  $\{*\prime\} = \text{perm}\{\underbrace{\circ \dots \circ}_{\nu_*+1}, \underbrace{\bullet \dots \bullet}_{\bar{\nu}_*-1}\}$  and  $\{*\prime\prime\} = \text{perm}\{\underbrace{\circ \dots \circ}_{\nu_*-1}, \underbrace{\bullet \dots \bullet}_{\bar{\nu}_*+1}\}$ , respectively.

As a result,

- Expression (2.4) for the knot invariant is expanded as a sum over the vertices of the directed graph, called a *resolution hypercube*<sup>5</sup>.

For example, Fig. 3 illustrates the hypercube for the diagram in Fig. 2.

**The generating function for the colourings** is defined as a formal series in the new variable  $T$  as follows

$$\mathfrak{Z}(q, T) \equiv \mathcal{Z}(\mathcal{R}(q) \rightarrow \mathfrak{R}(q, T)) = \sum_{* \in \{\circ, \bullet\}^n} T^{\nu_*} \mathcal{Z}, \quad \bar{\nu}_* = \#\{\bullet \in *\}, \quad (2.9)$$

where  ${}^*\mathcal{Z}$  stands for the expansion term related to the colouring  $*$ .

Expansion (2.9) is formally obtained from expression (2.4) for the knot invariant by substituting the crossing operators with

$$\begin{aligned} {}^+\mathfrak{R}(q, T) &\equiv q \circ \mathcal{R}(q) + T \bullet \mathcal{R}(q) \\ {}^-\mathfrak{R}(q, T) &\equiv q^{-1} \circ \mathcal{R}(q) + T \bullet \mathcal{R}(q), \end{aligned} \quad (2.10)$$

or, equivalently, their matrix elements with

$$\left\{ \begin{array}{l} \mathcal{R}_{ii}^{ii} \mapsto q, \quad 1 \leq i \leq 1, \\ \mathcal{R}_{ji}^{ij} \mapsto T, \quad 1 \leq i \neq j \leq N, \\ \mathcal{R}_{ij}^{ij} \mapsto q + q^{-1}T, \quad 1 \leq i < j \leq N, \\ \mathcal{R}_{ji}^{ji} \mapsto q(1 + T), \quad 1 \leq i < j \leq N, \end{array} \right. \quad \left\{ \begin{array}{l} \tilde{\mathcal{R}}_{ii}^{ii} \mapsto q^{-1}, \quad 1 \leq i \leq 1, \\ \tilde{\mathcal{R}}_{ji}^{ij} \mapsto T, \quad 1 \leq i \neq j \leq N, \\ \tilde{\mathcal{R}}_{ij}^{ij} \mapsto q^{-1} + qT, \quad 1 \leq i < j \leq N, \\ \tilde{\mathcal{R}}_{ji}^{ji} \mapsto q^{-1}(1 + T), \quad 1 \leq i < j \leq N. \end{array} \right. \quad (2.11)$$

<sup>5</sup>In the graphical representation for the tensor contractions, the expansion terms are associated with the various *resolutions* of the knot diagram.

## 2.4 Vector spaces at the hypercube vertices

The next step introduces representation theory data into the construction (see, e.g., [38] for the necessary background). The following presentation is equivalent to the standard presentation of the Khovanov construction [5] for the particular case of the  $\mathfrak{su}_2$  algebra (details can be found in [6]). It is very plausible that the KhR construction [4] in the more general case of  $\mathfrak{su}_N$  is also reproduced, although in somewhat different notions<sup>6</sup>.

**The operators related to a colouring.** The  ${}^*\bar{\mathcal{Z}}$  contribution to (2.4), related to the colouring  $*$  (with  $\nu_*$  resolutions  $\circ$ ,  $\bar{\nu}_*$  resolutions  $\bullet$ ,  $n = \nu_* + \bar{\nu}_*$  of them in total), identically equals to the contraction of two operators (we omit the operators  ${}^*\widehat{\mathcal{Q}}_j^i = {}^*\check{\mathcal{Q}}_j^i = \delta_j^i$ ). The first of these operators is given by

$$\mathcal{Q}^{\circ m} \Big|_J = \prod_{\substack{\curvearrowright \\ i \ j}} {}^*\check{\mathcal{Q}}_j^i \prod_{\substack{\curvearrowleft \\ i \ j}} {}^*\widehat{\mathcal{Q}}_j^i \quad (2.12)$$

where  $m$  is the number of the “left-to-right” turning points on the knot diagram<sup>7</sup> (those are the only turning points one takes into account). The second operator is

$${}^*\mathcal{Z}_J^I \equiv q^{\nu_+ - \nu_-} \prod_{\substack{\curvearrowright \\ i \ j \\ l \ k}} {}^\circ\mathcal{R}_{kl}^{ij} \prod_{\substack{\curvearrowleft \\ i \ j \\ l \ k}} \bullet\mathcal{R}_{kl}^{ij}, \quad * \in \{\circ, \bullet\}^n, \quad (2.13)$$

where we introduce the number  $\nu_+$  (resp.  $\nu_-$ ) of  $\curvearrowright$  (resp.  $\curvearrowleft$ ) crossings resolved into  ${}^\circ\mathcal{R}$

$$\nu_+ = \#\{\curvearrowright \rightarrow \curvearrowright \in \mathcal{D}^*\}, \quad \nu_- = \#\{\curvearrowleft \rightarrow \curvearrowleft \in \mathcal{D}^*\}. \quad (2.14)$$

The power of  $q$  factor appears as a price for expressing both  ${}^+\mathcal{R}$  and  ${}^-\mathcal{R}$  through the same pair  ${}^\circ\mathcal{R}$  and  $\bullet\mathcal{R}$ . The multi-indices  $I$  (resp.  $J$ ) are defined as the sets of the labels attached to the edges coming in (resp. going out of) the turning points, i.e.,

$$I = \left\{ \bigcup_{\substack{\curvearrowright \\ i \ j}} \bigcup_{\substack{\curvearrowleft \\ i \ j}} i \right\}, \quad J = \left\{ \bigcup_{\substack{\curvearrowright \\ i \ j}} \bigcup_{\substack{\curvearrowleft \\ i \ j}} j \right\}. \quad (2.15)$$

Hence, both operators  $\mathcal{Q}^{\circ m}$  and  ${}^*\mathcal{Z}$  are defined on the tensor power  $V^{\circ m}$  of the original space  $V$ ,  $m$  being the number of the “left-to-right” turning points in the knot diagram. In the following we also consider the composition of these two operators

$${}^*\bar{\mathcal{Z}} \equiv \mathcal{Q}\mathcal{Z}. \quad (2.16)$$

Contraction (2.4) can then be equivalently presented as a trace

$$\mathcal{H} = \text{Tr}_{V^{\circ m}} \mathcal{Q}\mathcal{Z} = \text{Tr}_{V^{\circ m}} \mathcal{Q}^{\circ m} \mathcal{Z} = \text{Tr}_{V^{\circ m}} {}^*\bar{\mathcal{Z}}. \quad (2.17)$$

<sup>6</sup>Two resolutions of a crossing in [4] are identified with two terms in the decomposition (2.8) for the  $\mathfrak{su}_N$   $\mathcal{R}$ -matrix in the fundamental representation [38]. Then the spaces in the vertices of the resolution hypercube (and hence the spaces in the resulting complex), are described in [4] as the complexes of certain commutative polynomial rings. At the same time, these complexes describe  $\mathfrak{su}_N$  representation spaces in terms of the BGG resolvents [39]. The author is indebted to I. Danilenko for pointing out this observation and providing the reference.

<sup>7</sup>Then the knot diagram has  $2m$  turning points in total. Indeed, the numbers of turning points of various kinds on a closed curve satisfy  $\begin{cases} \#\{\curvearrowright\} + \#\{\curvearrowleft\} = \#\{\curvearrowright\} + \#\{\curvearrowleft\} \\ \#\{\curvearrowright\} + \#\{\curvearrowleft\} = \#\{\curvearrowright\} + \#\{\curvearrowleft\} \end{cases}$ , and the sum (resp. difference) of these equations yields  $\#\curvearrowright = \#\curvearrowleft$  (resp.  $\#\curvearrowright = \#\curvearrowleft$ ).

## 2.5 Spaces at the vertices as graded spaces

The Khovanov [5] and the KhR [4] constructions both essentially use one more notion related to representation theory of quantum groups [38]. Namely, a special *graded* basis is considered in each vertex of the hypercube. Below we give the  $\mathcal{R}$ -matrix description of these spaces implicitly used for explicit computations in [3].

**Spaces at the vertices as image spaces.** One can show that<sup>8</sup>

$${}^*\bar{\mathcal{Z}}({}^*\bar{\mathcal{Z}}(\mathcal{V})) = {}^*\bar{\mathcal{Z}}(\mathcal{V}) \subset V^{\mathcal{D}}, \quad (2.18)$$

i.e., one can restrict the operator  ${}^*\bar{\mathcal{Z}}$ , originally defined on the space  $V^{om}$ , to its image where it acts as an isomorphism:

$$\boxed{{}^*\bar{\mathcal{Z}} : \mathcal{V}^* \equiv \text{Im } {}^*\bar{\mathcal{Z}}|_{V^{om}} \rightarrow \mathcal{V}^*} \quad (2.19)$$

Henceforth, we

- relate a colouring  $*$  to the space  $\mathcal{V}^*$  defined by (2.19), with  ${}^*\bar{\mathcal{Z}}$  defined in (2.13, 2.16) and put this space in the corresponding hypercube vertex.

**Basis of eigenvectors as a graded basis.** The operator  ${}^*\bar{\mathcal{Z}}$  has a basis of eigenvectors in the subspace  $\mathcal{V}^*$ , the eigenvalues being  $q$  powers,<sup>9</sup>

$$\{\mathcal{X}_\alpha^* : {}^*\bar{\mathcal{Z}}\mathcal{X}_\alpha^* = q^{\Delta_\alpha}\mathcal{X}_\alpha^*\}_{I=1}^{\dim \mathcal{V}^*}. \quad (2.20)$$

Hence, one can consider the linear space

$$v^* \equiv \text{span} \{q^{\Delta_\alpha}\}. \quad (2.21)$$

The contraction

$$\mathfrak{P}^*(q) \equiv \text{Tr}_{\mathcal{V}^*} {}^*\bar{\mathcal{Z}} \quad (2.22)$$

is then the generating function for the basis of monomials in  $q$ . The two-variable generating function,

$$\mathfrak{P}(q, T) \equiv \mathcal{H}(\mathcal{R} \rightarrow \mathfrak{R}) = \sum_* T^{\nu_*} \mathfrak{P}^*(q). \quad (2.23)$$

then coincides with the *primary polynomial* introduced in [3].

- Relations (2.22, 2.23) associate each term in the primary polynomial with a vector of the linear space placed at one of the resolution hypercube vertices.

---

<sup>8</sup> The operators  ${}^*\mathcal{R}$  ( $*$   $\in$   $\{\circ, \bullet\}$ ) defined in (2.8), satisfy  ${}^*\mathcal{R}^2 \sim {}^*\mathcal{R}$ , so that, if  $y \in \text{Im } {}^*\mathcal{R}$ , then  $y = {}^*\mathcal{R}^2 x = {}^*\mathcal{R} x \in {}^*\mathcal{R}(V)$  and hence the same is true for  ${}^*\mathcal{Z}$ , which by definition (2.13) is a tensor product of the operators  ${}^*\mathcal{R}$ . The same is also true for the operator  ${}^*\bar{\mathcal{Z}} = \mathcal{Q}^*\mathcal{Z}$ , because  $\mathcal{Q}^*\mathcal{Z} = {}^*\mathcal{Z}\mathcal{Q}$  for any  ${}^*\mathcal{Z}$  (due to the “built in” representation theory properties of these operators [38]) so that

$$x = \mathcal{Q}^*\mathcal{Z}(\mathcal{Q}^*\mathcal{Z}y) = \mathcal{Q}^*\mathcal{Z}^2 y \Rightarrow x = \mathcal{Q}^*\mathcal{Z}z = \mathcal{Q}^*\mathcal{Z}(\mathcal{Q}y),$$

and

$${}^*\bar{\mathcal{Z}}(\mathcal{V}) \equiv \mathcal{Q}^*\mathcal{Z}(\mathcal{V}) \subset {}^*\bar{\mathcal{Z}}^{-1}\mathcal{V} \subset \mathcal{V} \Rightarrow \mathcal{V} \subset {}^*\bar{\mathcal{Z}}\mathcal{V}$$

The relations above imply that the operator  ${}^*\bar{\mathcal{Z}}$  is invertible. Hence,  ${}^*\bar{\mathcal{Z}}(\mathcal{V}) = \mathcal{V}$ , as claimed.

<sup>9</sup> Similarly to the previous property, these facts follow from the definitions (2.13), (2.16) and the commutation relation  $\mathcal{Q}^*\mathcal{Z} = {}^*\mathcal{Z}\mathcal{Q}$ .

## 2.6 From the resolution hypercube to the complex

The last step of the Khovanov [5]/KhR [4] construction consists of relating the resolution hypercube arrows to certain maps (the *morphisms*). These maps must respect the graded bases associated with the hypercube vertices, and this severely constraints the form of the morphisms<sup>10</sup>.

The resolution hypercube is then transformed into the Khovanov/KhR complex in a canonical way [5, 4].

**Maps associated with edges as maps of the graded spaces.** An edge of the hypercube is by definition oriented from a colouring  $*$  to a colouring  $*'$  obtained by the change  $\circ \rightarrow \bullet$  at only one vertex of the knot diagram. The edge corresponds to a *morphism*, i.e., to a linear map

$$\mathfrak{M}_{*'}^* : \mathcal{V}^* \rightarrow \mathcal{V}^{*'} . \quad (2.24)$$

Here we do not determine this map explicitly<sup>11</sup>, but formulate an essential constraint on which we heavily rely in what follows<sup>12</sup>. Namely,

- The maps acting along the edges must commute with the maps  ${}^*\bar{\mathcal{Z}}$  of the spaces in the hypercube vertices,

$$\boxed{\mathfrak{M}_{*'}^* {}^*\bar{\mathcal{Z}} = {}^*\bar{\mathcal{Z}} \mathfrak{M}_{*'}^*} . \quad (2.25)$$

Relation (2.25) implies that an eigenvector  $\mathcal{X} \in \mathcal{V}^*$  of  ${}^*\bar{\mathcal{Z}}$ , is mapped to an eigenvector  $\mathcal{X}' \in \mathcal{V}^{*'}$  of  ${}^*\bar{\mathcal{Z}}$  with the same eigenvalue,

$${}^*\bar{\mathcal{Z}}\mathcal{X} = q^\Delta \mathcal{X} \Rightarrow {}^*\bar{\mathcal{Z}}\mathcal{X}' = {}^*\bar{\mathcal{Z}}\mathfrak{M}_{*'}^*\mathcal{X} = \mathfrak{M}_{*'}^*{}^*\bar{\mathcal{Z}}\mathcal{X} = q^\Delta \mathfrak{M}_{*'}^*\mathcal{X} = q^\Delta \mathcal{X}' . \quad (2.26)$$

The same statement in terms of the gradings introduced above reads:

- Morphism (2.24) maps a graded vector  $\mathcal{X} \in \mathcal{V}^*$  to the graded vector  $\mathcal{X}' \in \mathcal{V}^{*'}$  with the same grading<sup>13</sup>.

**The differentials compatible with the grading .** To obtain the complex, one should first construct a sequence of linear spaces that are direct sums of the spaces at separate hypercube vertices. Namely, the sum for the space  $\mathcal{V}_k$  includes all colourings with  $\nu_* = k$  instances of  $\bullet$ ,

$$\mathcal{V}_k = \bigoplus_{\nu_*=k} \equiv \mathcal{V}^* , \quad k = \overline{0, n} , \quad (2.27)$$

so that the space can be associated to the hypercube section spanned by the vertices with exactly  $\nu_* = k$  of the coordinates being equal to 0. The differential  $\hat{d}_k$  is then associated to the pair of the successive sections with  $k$  differing by 1. This operator acts from the space  $\mathcal{V}_{k-1}$  to the space  $\mathcal{V}_k$  as a sum of the corresponding morphisms (with proper signs),

$$\bigoplus_{\nu_*'=k+1}^{\nu_*=k} (-1)^{\text{par}^* + \text{par}^{*'}} \mathfrak{M}_{*'}^* \equiv \hat{d}_k : \mathcal{V}_k \rightarrow \mathcal{V}_{k+1}, \quad k = \overline{0, n-1}, \quad (2.28)$$

where  $\text{par}^* \in \{0, 1\}$  is the number of steps from the initial vertex  $\{\circ^n\}$  to the vertex  $*$  **modulo 2**. (two colourings thus have distinct parities, whenever differing by the only permutation  $\begin{smallmatrix} \bullet & \bullet \\ \circ & \circ \end{smallmatrix} \leftrightarrow \begin{smallmatrix} \circ & \bullet \\ \bullet & \circ \end{smallmatrix}$ ).

<sup>10</sup>The morphisms are described in [4] as ring homomorphisms.

<sup>11</sup>See [4] for the original definition, [22, 11] for adaptations to explicit computations, and [23] for an attempt to give an alternative definition.

<sup>12</sup>Some further properties of the maps are discussed in sec. 4

<sup>13</sup>In fact, only that a graded vector is mapped to a graded vector is essential, while the equality of the gradings ( $\Delta = \Delta'$ ) is related to the freedom in the definition of the morphisms (i.e., there are different possibilities that ultimately yield the same knot invariant). A more conventional choice (in particular, used in [5, 18, 4, 22, 19, 20, 23, 32]) is such that the morphisms lower the grading by one:  $\Delta' = \Delta - 1$ .

The differentials defined by (2.28) are by construction nilpotent,

$$\hat{d}_k \hat{d}_{k-1} = 0, \quad k = \overline{1, n}, \quad (2.29)$$

and commute with the colouring operators  ${}^* \bar{\mathcal{Z}}$  (because all the morphisms do),

$$\mathcal{Z}_{k+1} \hat{d}_k = \hat{d}_{k+1} \mathcal{Z}_k \quad \text{with} \quad \mathcal{Z}_k \equiv \bigoplus_{\nu_* = k} \mathcal{V}^*. \quad (2.30)$$

In other words,

- Starting from the resolution hypercube, the linear spaces at the vertices and the morphisms along the directed edges, one constructs a sequence of spaces associated with entire hyperplanes and sequence of nilpotent grading-preserving<sup>14</sup> linear maps, the *differentials*. The resulting sequence provides the *complex* [40] associated with the knot diagram.

## 2.7 Graded basis in the homologies

In Eq. (2.20) we introduced graded bases in the hypercube vertices. There is, however, a freedom in the definition of such a basis: one can make a linear transformation mixing the vectors of the same grading. Below we describe a special basis, which is the union of the graded bases in the image, co-image and the homology subspaces of the differentials in the complex. A more detailed derivation is given in B.

Nilpotency condition (3.2) implies that

$$x \in \text{Im } \hat{d}_k \subset \mathcal{V}_k \stackrel{\text{def}}{\Leftrightarrow} x = \hat{d}_k y \quad \Rightarrow \quad x \in \ker \hat{d}_{k+1} \subset \mathcal{V}_{k+1} \stackrel{\text{def}}{\Leftrightarrow} \hat{d}_{k+1} x = 0 \quad (2.31)$$

The converse is generally wrong. The homology space is by definition [40] the *factor space*

$$H_k \stackrel{\text{def}}{=} \ker \hat{d}_{k+1} / \hat{d}_k \subset \mathcal{V}_{k+1}, \quad \text{i.e.,} \quad x \in H_k \Leftrightarrow \hat{d}_k x = 0 \ \& \ \hat{d}_k y \neq x, \ \forall y \in \mathcal{V}_k, \quad (2.32)$$

i.e., each vector  $x$  in the homology  $H_k$  is a kernel vector defined up to an arbitrary vector from the image subspace,  $x \sim x + \hat{d}_k y, \forall y \in \mathcal{V}_k$ . Hence, one can identify the homology with any subspace  $H_k \in \ker \hat{d}_k$  of the kernel such that  $\dim H_k = \dim \ker \hat{d}_k - \dim \text{Im } \hat{d}_{k-1}$ .

Just using the definitions we have the decomposition

$$\mathcal{V}_k = \text{Im } \hat{d}_k \oplus \text{coIm } \hat{d}_{k+1} \oplus H_k, \quad (2.33)$$

where  $x \in \text{coIm } \hat{d} \stackrel{\text{def}}{\Leftrightarrow} \hat{d}x \neq 0$ .

A non-trivial consequence of the property (2.30) of the differentials is that

- Each of the three spaces in the decomposition (2.33) contains a graded basis.

Precisely, a basis in the space  $\mathcal{V}_k$  can be composed of three groups of vectors (see App. B),

$$\left\{ y_{k,i} : \hat{d}_{k+1} y_{k,i} \neq 0 \right\}_{i=1}^{\dim \text{Im } \hat{d}_{k+1}} \cup \left\{ z_{k,i} = \hat{d}_k y_{k-1,i} \right\}_{i=1}^{\dim \text{Im } \hat{d}_k} \cup \left\{ h_{k,i} \right\}_{i=1}^{\dim \mathcal{V}_k - \dim \text{Im } \hat{d}_k - \dim \text{Im } \hat{d}_{k+1}}, \quad (2.34)$$

$$\hat{\Delta} y_{k,i} = \Delta_{k,i} y_{k,i} \quad \hat{\Delta} z_{k,i} = \Delta_{k-1,i} z_{k,i} \quad \hat{\Delta} h_{i,k} = \Delta'_{i,k} h_{i,k}.$$

## 2.8 The geometric meaning of the positive integer decomposition

Here we address the final issue of this section, namely the derivation of the positive integer decomposition for the primary polynomial from [3].

<sup>14</sup>See the above footnote in the definition of the morphisms.

Calculating the trace (2.17) in the basis (2.34) yields the following decomposition of the generating function

$$\begin{aligned}
\mathfrak{P}(q, T) &= \sum_{k=0}^n T^k \text{Tr}_{\mathcal{V}_k} q^{\hat{\Delta}} \equiv \sum_{k=0}^n T^k \dim_q \mathcal{V} = \sum_{k=0}^n T^k \left( \text{Tr}_{\text{coIm } \hat{d}_{k+1}} q^{\hat{\Delta}} + \text{Tr}_{\text{Im } \hat{d}_k} q^{\hat{\Delta}} + \text{Tr}_{H_k} q^{\hat{\Delta}} \right) \stackrel{(2.34)}{=} \\
&= \sum_{k=0}^n T^k \left( \sum_{i=1}^{\dim \text{Im } \hat{d}_{k+1}} q^{\Delta_{k,i}} + \sum_{i=1}^{\dim \text{Im } \hat{d}_k} q^{\Delta_{k-1,i}} + \sum_{i=1}^{\dim H_k} q^{\Delta'_{k,i}} \right) = \\
&= \sum_{k=0}^{n-1} \left( T^k + T^{k+1} \right) \sum_{i=1}^{\dim \text{Im } \hat{d}_{k+1}} q^{\Delta_{k,i}} + \sum_{k=0}^n T^k \sum_{i=1}^{\dim H_k} q^{\Delta'_{k,i}} = (1+T) \mathcal{J}(q, T) + \mathcal{P}(q, T). \quad (2.35)
\end{aligned}$$

Note that the coefficient of each power  $q^{\Delta}$ , both in  $\mathcal{J}(q, T)$  and  $\mathcal{P}(q, T)$ , as well as in  $\mathfrak{P}(q, T)$ , is nothing but the multiplicity of the basis vector from the corresponding subspace ( $\oplus_{k=1}^n \text{Im } \hat{d}_k$ ,  $\oplus_{k=0}^n H_k$  or  $\oplus_{k=0}^n \mathcal{V}_k$ , respectively) with the grading  $\Delta$ . This leads to the essential property of the obtained decomposition,

- All three quantities in decomposition (2.35), the dividend  $\mathfrak{P}(q, T)$ , the quotient  $\mathcal{J}(q, T)$  and the remainder  $\mathcal{P}(q, T)$  are sums of the  $q$  and  $T$  powers with *positive integer* coefficients.

### 3 Minimal positive division instead of computing the homology

In this section, we wish to discuss the positive integer division approach as a shortcut in general homology computations, without reference to the knot theory applications.

Through the section, the spaces  $V$ , the maps  $\hat{d}$  and all the related quantities are not associated anyhow with the particular complexes arising from the knot theory. Here we do not consider graded linear spaces, since a graded complex (see sec. 2.5) is always a direct sum of ordinary complexes. Also we do not consider any additional structures on the linear spaces, such as the structure of Lie algebra representation (this is the case of the next section, sec. 4).

#### 3.1 General definitions

##### 3.1.1 Complex, homologies and decomposition of the generating functions.

Despite the fact that the most relevant definitions and theorems have already been given above, in sec. 2, we present them below in a compressed form for convenience.

Generally, a complex [40] is defined as a sequence of linear spaces and linear maps,

$$0 \xrightarrow{\hat{d}_0} V_0 \xrightarrow{\hat{d}_1} V_1 \xrightarrow{\hat{d}_2} V_2 \xrightarrow{\hat{d}_3} \dots \xrightarrow{\hat{d}_n} V_n \xrightarrow{\hat{d}_{n+1}} 0, \quad (3.1)$$

such that any pair of the subsequent maps satisfies the *nilpotency* condition:

$$\hat{d}_2 \hat{d}_1 = \hat{d}_3 \hat{d}_2 = \dots = \hat{d}_n \hat{d}_{n-1} = 0. \quad (3.2)$$

Condition (3.2) in particular implies that  $\text{Im } \hat{d}_k \subset \ker \hat{d}_{k+1}$  ( $k = \overline{0, n}$ ).

The homology in term  $k$  is the *factor space*

$$H_k \equiv \ker \hat{d}_{k+1} / \text{Im } \hat{d}_k, \quad (3.3)$$

which can be understood as a subspace of kernel vectors, in which any two vectors differing by an image vector are treated as the same homology element,

$$\begin{aligned}
x \in H_k &\Rightarrow \hat{d}_{k+1} x = 0, \\
x \sim y \in H_k &\Leftarrow \hat{x} - y = \hat{d}_k z \quad \left( \stackrel{(3.2)}{\Rightarrow} \hat{d}_{k+1} x = \hat{d}_{k+1} y = 0 \right).
\end{aligned} \quad (3.4)$$

The generating functions

$$\mathcal{F} \equiv \sum_{k=0}^n T^k \dim V_k, \quad \mathcal{J}(T) \equiv \sum_{k=0}^n T^k \dim \operatorname{Im} \hat{d}_k, \quad \mathcal{P} \equiv \sum_{k=0}^n T^k \dim H_k \quad (3.5)$$

in formal variable  $T$  for the dimensions of the linear spaces, the image subspaces and the homologies satisfy the relation (a particular case of (2.35), when  $q = 1$  so that  $\dim_q \rightarrow \dim$ )

$$\boxed{\mathcal{F}(T) = \mathcal{P}(T) + \mathcal{J}(T)(1 + T)}. \quad (3.6)$$

The function  $\mathcal{P}(T)$  is referred to as the *Poincare polynomial* of the complex; in particular,  $\chi \equiv \mathcal{P}(T = -1)$  is the *Euler character* of the complex. In the following, we call (3.6) a *positive integer decomposition* for the generating function, because

- All the coefficients of the  $T$  powers in  $\mathcal{F}(T)$ ,  $\mathcal{P}(T)$  and  $\mathcal{J}(T)$  are by definition positive integer numbers (the dimensions of the corresponding subspaces).

We study the following question:

- To what extent can one recover the remainder  $\mathcal{P}(T)$  from the dividend  $\mathcal{F}(T)$  **avoiding** the straightforward computing the homology?

The realization of the Strong expectation formulated in sec. 1.2 is associated with the progress along this way.

Treated as an isolated algebraic problem, the above question can possess no satisfactory answer, not being even formulated rigorously. Below we attempt to formulate the problem more precisely, employing various additional considerations.

### 3.1.2 Integer and polynomial division.

The polynomial division is a straightforward extension of the integer division<sup>15</sup>. Both problems are formulated in the table below (the given quantities are underlined, the quantities to be determined are marked by the question sign).

Integer division		Polynomial division (variable $T$ )	
$m, k, q, p \in \mathbb{Z}$		$\mathcal{F}(T), \mathcal{G}(T), \mathcal{J}(T), \mathcal{P}(T) \in \operatorname{Pol}(T)$	
$m$ <u>dividend</u>	$=$ <u>divisor</u>	$\cdot$ quotient	$+$ remainder
$k$	$q$	$+$	$p$
?	?	?	?
ambiguity		constraint	
$k \rightarrow q + u, \quad p \rightarrow p - ku, \quad u \in \mathbb{Z}$		$0 \leq p < q$	
$\mathcal{F}(T)$ <u>dividend</u>	$=$ <u>divisor</u>	$\cdot$ quotient	$+$ remainder
$\mathcal{G}(T)$	$\mathcal{J}(T)$	$+$	$\mathcal{P}(T)$
?	?	?	?
ambiguity		ambiguity	
$\mathcal{J} \rightarrow \mathcal{J} + f(T), \quad \mathcal{P} \rightarrow \mathcal{P} - f(T)Q, \quad f(T) \in \operatorname{Pol}(\mathbb{Z} T)$			

(3.7)

In both cases the equality in the third row does not define the unknown quantity uniquely. Namely, the equality still holds if both the quotient and the remainder are subjected to the transformation in the last row. In the integer case, the ambiguity is conventionally fixed by the constraint given in the same line. The polynomial case is essentially distinct at this point. Namely, none of the formal ways to select the unique remainder (now defined up to a polynomial instead of just an integer) *a priori* produces a quantity adequate for our purposes.

<sup>15</sup>It is in fact the *multivariable* division, which is applied to the KhR calculus, but we do not discuss this generalization here.



### 3.1.3 Division as homology computation

Now we give an elementary illustration of the main idea we use, namely of the correspondence between the homology calculus and the polynomial division, with a freedom in definition of the remainder (see the last line in Tab. 3.7 and the comment in the end of sec. 3.1.2). Below we take a simple particular case of division problem, and construct two different complexes with the homologies producing two different remainders.

In the context of knot polynomials (see sec. 6), we in fact deal with the very special case of the right column of Tab. 3.7, when all the polynomials have only positive integer coefficients, and the divisor is the binomial  $(1 + T)$ . The general problem we consider is to present a given polynomial  $\mathcal{F}(T)$  in the form

$$\boxed{\mathcal{F}(T) = (1 + T)\mathcal{J}(T) + \mathcal{P}(T)} \quad (3.8)$$

$$\mathcal{F}(T) = \sum_{k=0}^n a_k T^k, \quad \mathcal{J}(T) = \sum_{k=0}^m b_k T^k, \quad \mathcal{P}(T) = \sum_{k=0}^l c_k T^k, \quad \{a_k, b_k, c_k\} \subset \mathbb{Z}_+.$$

Large freedom in the definition of the remainder yet remains even in this particular case, as we will see in the examples below.

In the particular case described below the division problem is straightforwardly related to the problem of computing the homologies. Namely, extracting the  $\sim (1 + T)$  part is equivalent to matching the monomial terms in the pairs  $(x, Tx)$ , each monomial entering only one pair. Some monomials remain unpaired and represent the homologies. E.g.,  $\mathcal{F}(T) = 3 + 4T + T^2$  admits two matchings, each with one unpaired monomial,

$$\begin{array}{c} \underline{3 + 4T + 2T^2} = \\ \begin{array}{c} 3 + 3T \\ + T + T^2 \\ \bullet \longrightarrow \bullet + \boxed{T^2} \\ \bullet \longrightarrow \bullet \\ \bullet \longrightarrow \bullet \hat{d}_1 \\ \hat{d}_0 \bullet \longrightarrow \bullet \\ \bullet \end{array} \quad \left| \quad \begin{array}{c} 1 + \\ 2 + 2T \\ \bullet + 2T + 2T^2 \\ \bullet \longrightarrow \bullet \\ \bullet \longrightarrow \bullet \hat{d}_1 \\ \hat{d}_0 \bullet \longrightarrow \bullet \\ \bullet \longrightarrow \bullet \end{array} \right. \\ \hline (1 + T) \cdot (3 + T) + \boxed{T^2} \quad \left| \quad \boxed{1} + (2 + 2T) \cdot (1 + T) \end{array} \quad (3.9)$$

In either diagram in (3.9), a bullet is placed in the column  $(k + 1)$  for each  $T^k$  term in  $\mathcal{F}$ ; the arrows label the matching pairs. The positions of the arrows matching column  $k$  with column  $(k + 1)$  can then be represented by the matrix  $\hat{d}_{k-1}$  such that  $\hat{d}_{k-1}^{ij} = 1$  if bullet  $i$  in column  $k$  matches bullet  $j$  in column  $(k + 1)$ , and  $\hat{d}_{k-1}^{ij} = 0$  otherwise. Then, the two particular diagrams in (3.9) give rise to the matrices

$$\hat{d}_1 = \begin{pmatrix} 0 & 0 & 0 & 1 \\ 0 & 0 & 0 & 0 \\ 0 & 0 & 0 & 0 \end{pmatrix}, \quad \hat{d}_0 = \begin{pmatrix} 1 & 0 & 0 \\ 0 & 1 & 0 \\ 0 & 0 & 1 \\ 0 & 0 & 0 \end{pmatrix}, \quad \text{and} \quad \hat{d}_1 = \begin{pmatrix} 0 & 0 & 1 & 0 \\ 0 & 0 & 0 & 1 \end{pmatrix}, \quad \hat{d}_0 = \begin{pmatrix} 0 & 1 & 0 \\ 0 & 0 & 1 \\ 0 & 0 & 0 \\ 0 & 0 & 0 \end{pmatrix}. \quad (3.10)$$

In both cases  $\hat{d}_1 \hat{d}_0 = 0$ , since each bullet enters no more than one pair. Hence, if a column is associated with a linear space (and bullet with a basis vector), the arrows define the differentials with the matrices (3.10). One thus obtains the complex, with the homology spanned by the basis vectors corresponding to the unpaired bullet (related to the remainder in the division problem).

## 3.2 “Ambiguous” and “unambiguous” minimal remainders

As already discussed in sec. 3.1.2, decomposition (3.8) is not unique. The first and the most naive constraint we impose on the remainder is

- The remainder  $\mathcal{P}(T)$  contains the minimal possible number of different  $T$  powers.

Although this requirement defines the unique remainder only in particular cases, it turns out to be very useful in application to knot polynomials (see [3] and sec. 6). Moreover, all further more involved constraints will be developments of this elementary one.

Below we consider in details the simplest examples, when  $\mathcal{F}(T)$  contains up to three subsequent  $T$  powers<sup>16</sup>. The ambiguity in the remainder depends on the coefficients in the dividend. Explicit relations are provided in Tabs.<sup>17</sup> (3.11–3.12) (3.11), (3.12). As one can see from Tab. (3.12), already the case of the three-term dividend appears to be rather non-trivial.

$\mathcal{F}(T) = aT^k$	
Type	Unambiguous
$\mathcal{J}(T)$	0
$\mathcal{P}(T)$	$a_0T^k$

$\mathcal{F}(T) = a_0 + a_1T, \quad \chi \equiv a_0 - a_1$			
Type	Unambiguous		
Case	$\chi > 0$	$\chi = 0$	$\chi < 0$
	$\chi + a_1(1+T)$	$a_0(1+T)$	$(-\chi)T + a_0(1+T)$
$\mathcal{J}(T)$	$a_1$	$a_0 = a_1$	$a_0$
$\mathcal{P}(T)$	$\chi$	0	$(-\chi)T$

(3.11)

$\mathcal{F}(T) = a_0 + a_1T + a_2T^2, \quad \chi \equiv a_0 - a_1 + a_2$					
Type	Unambiguous			Ambiguous	
Case	$\chi \leq 0$	$\chi > 0$			
		$a_0 \leq a_1 < a_2$	$a_2 \leq a_1 < a_0$	$a_1 < a_0, a_1 < a_2$	$a_0 \leq a_1, a_2 \leq a_1$
$\mathcal{J}(T)$	$a_0 + a_2T$	$a_0 + (a_1 - a_0)T$	$(a_1 - a_2) + a_2T$	$(a_0 - p) + (p - a_0 + a_1)T$	$(a_1 - a_2) + a_2T;$ $a_0 + (a_1 - a_0)T$
$\mathcal{P}(T)$	$(-\chi)T$	$\chi T^2$	$\chi$	$p + (\chi - p)T^2$	$\chi;$
				$0 < a_0 - a_1 \leq p \leq a_0 < \chi$	$\chi T^2$
E.g.	$1 + 3T + T^2$	$1 + T + 2T^2$	$2 + T + T^2$	$3 + 2T + 4T^2 =$	$3 + 4T + 2T^2 =$
	$= T + (1+T)^2$	$= T^2 + (1+T)^2$	$= 1 + (1+T)^2$	$(1 + 4T^2) + 2(1+T)$ $= (2 + 3T^2) + (1+T)^2$	$T^2 + (1+T)(1+2T)$ $= 1 + 2(1+T)^2$

(3.12)

### 3.3 Properties of maps as “selection rules” for the “minimal remainder”

In this section we recall the homology computation problem (formulated in Sec. 3.1.1) underlying the minimal positive division problem we consider (formulated in Sec. 3.1.2). Below we explore, in the simplest cases, how the particular known properties of the differentials may help to determine the “minimal remainder”, when it is ambiguous.

#### 3.3.1 Ranks of the differentials

The maps  $\hat{d}$  in complex (3.1) can not be isomorphisms for generic dimensions of the spaces  $V$ . E.g., in the case of a two-term complex,

$$0 \xrightarrow{\hat{d}_0} V_0 \xrightarrow{\hat{d}_1} V_1 \xrightarrow{\hat{d}_2} 0, \quad (3.13)$$

the rank of the only non-zero map  $\hat{d}_1$  must satisfy

$$\text{rank } \hat{d}_1 \equiv \dim \text{Im } \hat{d}_1 \subseteq V_1 \leq \min(\dim V_0, \dim V_1). \quad (3.14)$$

<sup>16</sup>If the  $T$  powers are not subsequent, i.e.,  $a_k = 0$  for some  $k$ , then problem (3.8) should be solved separately for the polynomials  $\mathcal{F}'(T) = \sum_{k'=0}^{k-1} a_{k'}$  and  $\mathcal{F}''(T) = \sum_{k'=1}^n a_{k'}$  (such that  $\mathcal{F}(T) = \mathcal{F}'(T) + \mathcal{F}''(T)$ ); this is a consequence of the positive coefficients requirement.

<sup>17</sup>In the latter two cases we omit the inessential  $T$  power factor in  $\mathcal{F}$  by setting the smallest  $T$  power to zero.

Starting from the next case of a three-term complex,

$$0 \xrightarrow{\hat{d}_0} V_0 \xrightarrow{\hat{d}_1} V_1 \xrightarrow{\hat{d}_2} V_2 \xrightarrow{\hat{d}_3} 0, \quad (3.15)$$

the nilpotency condition also becomes non-trivial, producing additional constraints. In particular,  $\hat{d}_2\hat{d}_1 = 0$  implies that

$$\text{Im } \hat{d}_1 \subset \ker \hat{d}_2 \Rightarrow \text{rank } \hat{d}_1 \equiv \dim \text{Im } \hat{d}_1 \leq \dim \ker \hat{d}_2 = \dim V_1 - \dim \text{Im } \hat{d}_2 \equiv \dim V_1 - \text{rank } \hat{d}_2, \quad (3.16)$$

i.e.,

$$\text{rank } \hat{d}_1 + \text{rank } \hat{d}_2 \leq \dim V_1, \quad (3.17)$$

and also

$$\text{rank } \hat{d}_1 \leq \min(\dim V_0, \dim V_1), \quad \text{rank } \hat{d}_2 \leq \min(\dim V_1, \dim V_2), \quad (3.18)$$

similarly to the previous case.

The ranks of the differentials for various choices of minimal remainders in the division problem (3.11–3.12) are given in Tables (3.19), (3.20) (we omit the trivial one-term case).

dim $V_0 = v_0$ , dim $V_1 = v_1$ , $\chi = v_0 - v_1$			
Case	$\chi > 0$	$\chi = 0$	$\chi < 0$
max rank $\hat{d}_1$	$v_0$	$v_0 = v_1$	$v_1$
min dim $H_0 \subset V_0$	0	0	$-\chi$
min dim $H_1 \subset V_1$	$\chi$	0	0

(3.19)

dim $V_0 = v_0$ , dim $V_1 = v_1$ , dim $V_2 = v_2$ , $\chi = v_0 - v_1 + v_2$						
Case	$\chi \leq 0$	$\chi > 0$				
		$v_0 \leq v_1 < v_2$	$v_2 \leq v_1 < v_0$	$v_1 < v_0, v_1 < v_2$	$v_0 \leq v_1, v_2 \leq v_1$	
rank $\hat{d}_1$	$v_0$	$v_0$	$v_1 - v_2$	$v_0 - p$	$v_1 - v_2$	$v_0$
rank $\hat{d}_2$	$v_2$	$v_1 - v_0$	$v_2$	$p - v_0 + v_1$	$v_2$	$v_1 - v_0$
dim $H_0$	0	0	$\chi$	$0 < v_0 - v_1 \leq p \leq v_0$		0
dim $H_1$	$-\chi$	0	0	0		0
dim $H_2$	0	$\chi$	0	$0 < v_2 - v_1 \leq \chi - p$		$\chi$

(3.20)

### 3.3.2 Particular values of matrix elements

More detailed data include the values of the particular matrix elements. To determine explicitly just several of them it is sufficient to determine the ranks of the differentials, and hence the “minimal remainder”. For example,

$$\text{rank} \begin{pmatrix} k & k \end{pmatrix} = \begin{cases} 0, & k = 0 \\ 1, & k \neq 0 \end{cases}; \quad \text{rank} \begin{pmatrix} 1 & -1 & k \\ -1 & 1 & p \end{pmatrix} = \begin{cases} 0, & k + p = 0 \\ 1, & k + p \neq 0 \end{cases} \quad (3.21)$$

However, the general case is different, e.g.,

$$\forall k \text{ rank} \begin{pmatrix} 1 & k \end{pmatrix} = 1; \quad \forall k \text{ rank} \begin{pmatrix} 1 & -1 & k \\ -1 & 1 & 1 - k \end{pmatrix} = 2; \quad \forall k \text{ rank} \begin{pmatrix} 1 & -1 & k \\ -1 & 1 & -k \end{pmatrix} = 1; \quad (3.22)$$

$$\forall k, p \text{ rank} \begin{pmatrix} 1 & 0 & k \\ 0 & 1 & p \end{pmatrix} = 2.$$

### 3.4 “Multilevel” division as a way to fix ambiguities

A further “improvement” consists in artificially splitting the initial division problem into two (or more) levels. Namely, suppose the original polynomial is given in the form of the decomposition (the summation index  $Y$  running over a given set of values)

$$\mathcal{F}(T) = \sum_Y \mathcal{F}_Y(T) C_Y(T). \quad (3.23)$$

Then, the division can be first performed for each  $\mathcal{F}_Y(T)$  separately, and then for the linear combinations of the resulting remainders, namely

$$\text{I. } \mathcal{F}_Y(T) = \mathcal{P}_Y(T) + (1+T)\mathcal{J}_Y(T). \quad (3.24)$$

$$\text{II. } \mathcal{P}_I(T) \equiv \sum C_Y(T)\mathcal{P}_Y(T) = \mathcal{P}_{II}(T) + (1+T)\mathcal{J}_{II}(T). \quad (3.25)$$

The simplest example below illustrates how such “multilevel” division may fix an ambiguous remainder.

Let  $\mathcal{G}(T) = 1 + T$  and

$Y$	1	2
$C_Y$	1	$T^2$
$\mathcal{F}_Y$	$1+T$	1

(3.26)

so that  $\mathcal{F}(T)$  admits two positive integer decompositions, both with the monomial remainder,

$$\mathcal{F}(T) = \mathcal{F}_1 C_1 + \mathcal{F}_2 C_2 = 1 + T + T^2 = 1 + (1+T) \cdot T = T^2 + 1 \cdot (1+T). \quad (3.27)$$

From the viewpoint of the multilevel division, one decomposition is preferred, namely,

$$\begin{aligned} \text{I. } & \mathcal{F}_1 = 0 + 1 \cdot (1+T) \Rightarrow \mathcal{P}_1 = 0, \\ & \mathcal{F}_2 = 1 + 0 \cdot (1+T) \Rightarrow \mathcal{P}_2 = 1. \\ \text{II. } & \mathcal{P} = \mathcal{P}_1 C_1 + \mathcal{P}_2 C_2 = 0 \cdot 1 + 1 \cdot T^2 = T^2 + 0 \cdot (1+T) \Rightarrow \boxed{\mathcal{P}_{II} = T^2}. \end{aligned} \quad (3.28)$$

The suggested algorithm is motivated by the known properties of the knot polynomials, see [3] and sec. 5.

## 4 Lie algebra structure in the complex and its breaking

In this section, we return to the particular complex that arises in the context of knot invariants, associated with the resolution hypercube (see sec. 2.3), and discuss in some further details the spaces at the vertices and the morphisms along the edges.

Namely, we slightly touch the topic of representation theory structures associated with the resolution hypercube, with the constructed complex, and with the obtained knot invariants. Although at the moment we are able neither to present a closed construction, nor to extract any practical output, we see at least two reasons for addressing this subject.

First, the description of the spaces and differentials in the original KhR formalism [4, 22] refers to the representation theory (see ssec. 2.4–2.6, especially footnote<sup>6</sup>). In particular, it looks highly plausible that the representation theory properties of the morphisms determine their particular form to much extend.

Second, the known properties of the resulting knot invariants, which are the KhR invariants, as well as that of the closely related superpolynomials [10, 12], might have a natural representation theory interpretation. Moreover, it seem that this structure becomes more transparent, from the viewpoint of the differential expansion technique [28], and the evolution method [25] (see sec. 5).

In this section, we use a number of representation theory notions and statements without any comments, referring the reader to [38], whenever necessary. The most necessary notions are contained in the following

**Quick reference. Standard basis in the Lie algebra and in the representation space.** By definition, the Lie algebra  $\mathfrak{g}$  is a linear space (usually over complex numbers) with the additional operation (the *commutator*). I.e., any pair of elements  $A_1$  and  $A_2$  of the algebra correspond an element  $[A_1, A_2]$  of the algebra. Here we consider only simple finite dimensional Lie algebras.

In this case all elements of an algebra  $\mathfrak{g}$  can be obtained from the  $2r$  *generators*, by taking successively the commutators and linear combinations of the elements. The generators include lowering operators  $E_\alpha$  and the raising operators  $F_\alpha$ , with  $\alpha = \overline{1, r}$ .

A representation of the algebra is a linear map of the algebra to the space of linear operators consistent with the definition of the commutator. These linear operators act in the *representation space*  $V$  of the algebra. Throughout the text we consider the algebra together with its representation and do not make a difference between the algebra elements and the corresponding linear operators.

We consider only the finite-dimensional representations of simple Lie algebras. All these representations are *highest weight* representations. This means that the representation space contains the special basis composed of the highest vector  $X_\emptyset \equiv X$ , which is annihilated by all the raising operators ( $F_\alpha X = 0$ ,  $\alpha = \overline{1, r}$ ) and the maximum linearly independent subset of descendant vectors  $X_{\{\alpha\}} = E_{\alpha_1} \dots E_{\alpha_k} x$ , obtained from the successive action of the lowering operators on  $x$ . The vectors  $X_{\{\alpha\}}$  are the common eigenvectors of the *Cartan operators*  $H_\alpha = [E_\alpha, F_\alpha]$ , i.e.,  $H_\alpha X_{\{\beta\}} = \Lambda_{\alpha\{\beta\}} X_{\{\beta\}}$  for all possible  $\alpha$  and  $\{\beta\}$ .

For further details see, e.g., [38].

## 4.1 The idea

As we discussed in sec. 2, both the HOMFLY and the KhR invariants can be considered as the generating functions for the graded bases in the spaces in the Khovanov complex and in its homologies, respectively. The HOMFLY invariant is explicitly expressed through the  $\mathcal{R}$ -matrices, associated with certain Lie algebra representations, and can be expanded over the characters of these representations. This is not true for the KhR invariant. Yet, in particular cases these invariants can be expressed via some remnants of the representation theory structure that governs the HOMFLY polynomial [12], [25], [27], [28], [29], [23], [3], [?]. This phenomenon finds a natural explanation, if the spaces  $\mathcal{V}_k$  in the KhR complex are representation spaces of the Lie algebra, while the homologies are not. At the same time the latter ones can be invariant spaces of some subalgebra. In turn, this happens if the morphisms in the complex commute with this subalgebra, but not with the entire algebra.

## 4.2 Spaces in the resolution hypercube as representation spaces

In sec. 2 we describe the space  $\mathcal{V}^* \subset V^{om}$  at the hypercube vertex  $*$  as a subspace of the tensor power of the representation space  $V$  initially associated with the knot (the power  $m$  is half the number of the turning points on the knot diagram, see ssec. 2.4–2.5 including the footnote<sup>7</sup>). Precisely, these spaces are defined as invariant spaces of the grading operator  ${}^*\bar{\mathcal{Z}}$ , which allows one to introduce the graded basis  ${}^*\bar{\mathcal{Z}}$  of eigenvectors in each of these spaces (see tab. 4 for the basic formulas and for the general plan of the construction). Each space  $V_k$  in the complex is in turn defined as a direct sum of several  $\mathcal{V}^*$ ; hence, the  $\mathcal{V}_k$  is an invariant space of  ${}^*\bar{\mathcal{Z}}$  and has a graded basis as well. In this section, we consider an even stronger claim that

- The spaces in the complex constructed for a given knot are representation spaces of the Lie algebra  $\mathfrak{g}$  associated with the knot.

Note that  $\mathcal{V}^*$  is generally a **reducible** representation.

The above claim follows from the definition (2.12–2.16) of the operator  ${}^*\bar{\mathcal{Z}}$ , which is a contraction of the operators  $\mathcal{Q}$  and  $\mathcal{R}$ , and from the representation theory properties of these operators [38] (see also App. A). The derivation is similar to the reasoning in footnote<sup>8</sup>.

Since  $\mathcal{Q}$  and  $\mathcal{R}$ , and hence  ${}^*\bar{\mathcal{Z}}$  commute with all the elements of the algebra, i.e.,

$$A {}^*\bar{\mathcal{Z}} = {}^*\bar{\mathcal{Z}} A, \quad \forall A \in \mathfrak{g}, \quad * \in \{\circ, \bullet\}^n, \quad (4.1)$$

then

$$\forall x \in \mathcal{V}^* \left( \Leftrightarrow x = {}^*\bar{\mathcal{Z}}y \right) \Rightarrow Ax = {}^*\bar{\mathcal{Z}}(Ay) \in \mathcal{V}^*. \quad (4.2)$$

Hence, by definition,  $\mathcal{V}^*$  is the representation space of  $\mathfrak{g}$ , and the same is true for the sums of  $\mathcal{V}^*$  that yield  $\mathcal{V}_k$ .

### 4.3 Are the homology spaces representation spaces?

If the original spaces  $\mathcal{V}_k$  in the Khovanov complex are invariant spaces a linear operator  $A$ , then the homology spaces  $H_k$  must as well be invariant space of  $A$  if the operator commutes with the differential,  $A\hat{d}_k = d_k A$  (as we demonstrated in sec. 2.7 for  $A = {}^*\bar{\mathcal{Z}}$ ). However, the homology spaces may *not* be the invariant spaces of the operator  $A$  generally.

The actual properties of the KhR complexes are nicely compatible with the following picture. Assume that the differentials in the complex satisfy  $\hat{d}_k E_\alpha = E_\alpha \hat{d}_k$  and  $\hat{d}_k H_\alpha = H_\alpha \hat{d}_k$  for all  $\alpha = \overline{1, r}$ , but  $\hat{d}_k F_\alpha \neq F_\alpha \hat{d}_k$ , at least for some alpha. Applying these relations when the operators act on an arbitrary vector  $x \in \mathcal{V}_k$ , one concludes that

- The image of the Cartan eigenvector **must** be a Cartan eigenvector with the **eigenvalue**,

$$H_\alpha x = \lambda x \Rightarrow H_\alpha \hat{d}_k x = \lambda \hat{d}_k x. \quad (4.3)$$

- The image of a descendant of a vector **must** be the same descendant of the image of the vector,

$$\hat{d}_k (E_{\alpha_i} \dots E_1 x) = E_{\alpha_i} \dots E_1 \hat{d}_k x. \quad (4.4)$$

- The image of the highest vector may **not** be a highest vector,

$$F_\alpha x = 0 \not\Rightarrow F_\alpha \hat{d}_k x = 0. \quad (4.5)$$

The operators  $E_\alpha$  and  $H_\alpha$ , which satisfy the commutation relations  $[E_\alpha, H_\beta] = c_{\alpha\beta} E_\alpha$  (for some constants  $c_{\alpha\beta}$ ) [38], generate the subalgebra  $\mathfrak{g}'$  of the original Lie algebra  $\mathfrak{g}$ . Similarly, one consider the differentials that commute with all  $F_\alpha$  and  $H_\alpha$ , but not with all  $F_\alpha$ . In the both cases we obtain the following non-trivial property of the KhR construction,

- The homology spaces are generally **not** representation spaces of  $\mathfrak{g}$ .

Yet,

- The homology are invariant spaces of the subalgebra of  $\mathfrak{g}' \subset \mathfrak{g}$  that is respected by action of the differentials.

In particular, the grading operator  ${}^*\bar{\mathcal{Z}}$  can be an element of the *universal enveloping* [38] of  $\mathfrak{g}'$ , e.g.,  ${}^*\bar{\mathcal{Z}} = q^{\sum_{\alpha=1}^r H_\alpha}$ . Then the operators  ${}^*\bar{\mathcal{Z}}$  commute with the differentials as well, and hence in full consistence with sec. 2.7,

- The homology spaces are graded spaces.

The algebras generated by the  $2r$  operators  $E_\alpha$  (or  $F_\alpha$ ) and  $H_\alpha$  with  $\alpha = \overline{1, r}$ , are by the moment less studied, than simple Lie algebras generated by all  $3r$  operators  $E_\alpha$ , and  $F_\alpha$ , and  $H_\alpha$ . Yet, representations of the former algebras already reveal some inspiring properties. An particular, the characters of certain representations reproduce the MacDonalld polynomials at special point <sup>18</sup> [41]. The same polynomials at an other special point often can be used as an expansion basis for the knot superpolynomials [24].

---

<sup>18</sup>The author is indebted to S.Arthamonov for pointing out this reference.



## 5 Differential expansion and evolution method

### 5.0.1 The sketch of the methods

Now we briefly outline two more (highly interrelated) approaches to the KhR (and super-) polynomials. These two approaches are the *evolution method* [24, 25, 26] and the *differential expansion*<sup>19</sup> [12, 25, 27, 28, 29]. Some grounds for these approaches are given by recently obtained recurrent relations for the KR polynomials. In some cases these relations are derived from the Khovanov/KhR construction (essentially, from the exact skein triangle) [42, 43], while in other cases they remain an empiric observation. Hence, at the moment neither the differential expansion, nor the evolution method are based on any rigorously formulated construction. Yet both methods are highly effective as computational tools.

All three approaches — positive division, differential expansion and evolution method — share more in common with each other than with the original KhR construction. We include this issue in this section to emphasize the possible (as yet mostly empiric) relation of these approaches to Lie group representation theory. We complete the discussion by comparing the two approaches with the positive division approach (an interplay was already observed in [3]).

In both the evolution and the differential expansion methods one studies an entire family of knots instead of its single representative. The family can be either relatively general one, such as all knots that are the closures of three-strand braids, or a more restricted one, e.g., the knots obtained from a given one by performing subsequently a certain transformation. One then writes the desired knot invariant in the form

$$\text{Inv}^{\mathcal{K}}(q, T) = \sum_Y \text{Inv}_Y^{\mathcal{K}}(q, T) C_Y(q, T), \quad (5.1)$$

where  $Y$  is a summation index (e.g., an integer, or a partition) running over a finite (and “small”) set. The quantities  $C_Y$  are treated as the common “expansion basis” for the knot family, while the “expansion coefficients”  $\text{Inv}_Y$  are either (relatively) simple functions of parameter(s) inside the family, or at least have a much simpler form than the resulting sum. Moreover, the “expansion basis” usually consists of the products of some simple functions of an integer  $k$  (or, more generally, of a set of integers),

$$C_Y(q, T) = \frac{\prod_{k \in \phi \subset \mathbb{Z}} f^Y(k|q, T)}{\prod_{l \in \psi \subset \mathbb{Z}} g^Y(l|q, T)} \quad (5.2)$$

By construction, expansion (5.1) for  $T = -1$  must reproduce one of the known similar expansions for the HOMFLY polynomial (e.g., the character expansion [36, 33]). The factors in the “expansion basis” in this limit often become certain representation theory quantities (e.g., the quantum dimensions of the irreducible representation spaces, see sec. 4.2), and the expansion factors typically take form of the *quantum numbers*  $[n]_q \equiv \frac{q^n - q^{-n}}{q - q^{-1}}$  in the variable  $q$ . If this is the case, a typical “deformation” of the expansion for general  $T$  consists in the substitution

$$f_k^Y(q, T = -1) = [n_k]_q \equiv \frac{q^{n_k} - q^{-n_k}}{q - q^{-1}} \quad \longrightarrow \quad f_k^Y(q, T) = [n_k]_q \equiv \frac{q^{n_k} + q^{-n_k} T}{q + q^{-1} T}, \quad (5.3)$$

for some integer  $n_k$ . In many cases, the denominators cancel out, so that the answer takes form of a polynomial expanded over the ring generated by  $\{(q^{n_k} + Tq^{-n_k})\}$  (the generators are referred to as “differentials” in [28, 12, 25]).

### 5.0.2 The interplay with the positive division method

The observations on the structure of the KhR polynomials, which we summarised above, in fact motivated us to formulate the multi-level division algorithm (sec. 3.4). Namely, were the KhR invariants obtained

<sup>19</sup>See also discussion in [3], where, in particular, the relations between the variables used in different cited papers are explicitly written down.



merely by the first-level division, one could just identify  $C_Y$  and  $\mathcal{P}_Y$  in (3.25) with  $c_Y(q, T)$  and  $\text{Inv}_Y$  in (5.1), respectively. In the actual, more complicated case, initial structure (3.23) is broken down by the second-level division. Yet, one can observe some traces of this structure in the resulting invariant, which still can be written in the form (5.3).

### 5.0.3 The interplay with the group theory viewpoint



The quantities (5.3) usually look like “ $T$ -deformations” of some quantum dimensions. This observation might signal that they (similarly to their undeformed counterparts at  $T = -1$ ) are somehow related to the Lie algebra  $\mathfrak{g}$ , which acts on the spaces in the complex (see sec. 2, 4). The highest expectation would be that the  $C_Y(q, T)$  are invariants of the subalgebra  $\mathfrak{g}' \subset \mathfrak{g}$  that commutes with the action of the differentials (see also discussion and examples in sec. 4). In this case the KhR invariants could be explicitly computed as traces over the homology spaces of some linear operators, or at least somehow expressed in terms of such quantities.

## 6 Minimal positive division approach and CohFT calculus

In this section we turn to another point of view on the KhR calculus which appeared recently. This new approach is the soliton counting technique developed in [1, 2], which is part of the general framework of CohFT introduced in [14]. We do not go into the field theory background, concentrating on the details of practical computations instead. We mostly aim to compare this approach to the KhR invariants with the approach discussed in ssec. 2–4.

### 6.1 Preliminary comments

#### 6.1.1 CohFT diagram technique

Generally, the CohFT diagram is a knot diagram (see the definition in sec. 2.1), with a spin state (+ or –) assigned to each edge, and with (several kinds of) solitons distributed over the crossings and turning points of the knot diagram. Various possible diagrams can then be organized into a graph, similar to the resolution hypercube with various colourings in the vertices (sec. 2). However, one cannot distribute the solitons (playing the roles of two colourings  and ) at different crossings arbitrarily (see the particular examples below). Hence, the resulting graph is not simply a hypercube, and we will not describe it explicitly.

In the original CohFT construction [14, 1, 2], the diagrams span certain vector spaces. These spaces are used as building blocks to construct a complex, the differentials being defined by their matrix elements labelled by pairs of diagrams. The general idea is thus similar to that of the Khovanov [5, 18] and KhR [4, 22] constructions.

#### 6.1.2 Selection rule for CohFT matrix elements

To each CohFT diagram one can associate an integer, which is preserved by the differentials. Also in the basis associated with CohFT diagrams

- All the differentials in the constructed complex have matrix elements equal either to 0, or to 1, or to –1.

In other words, the CohFT diagrams enumerate the basis vectors, and play the role of grading considered in sec. 2.7. We recall (see sec. 2.8) that these bases give rise to the positive integer decomposition for the generating function (on a deeper level this relation follows from the structure of the differentials). The generating function for the basis vectors of the homology spaces (which gives the desired knot invariant) is then the remainder of division of the original (polynomial) generating function by a certain polynomial. Hence, a similar decomposition can be written down in terms of the CohFT diagrams.

### 6.1.3 Types of CohFT matrix elements and multilevel division

General considerations together with intuition from case studies result in further specification of the selection rules. In particular, the differentials the distribution of signs over the strands at the bottom of the braid appear to be especially simple.

- The morphisms responsible for the transitions between the soliton diagrams with the same initial spin state commute with the whole Lie algebra (associated with the gauge group),

and hence

- The matrix element of the differential between any pair of soliton diagrams with the same  $q$  grading and the  $T$  gradings differing by 1 equals either 1 or -1.

In the language of the minimal positive division this implies (see sec. 2.8) that, roughly speaking, the corresponding terms in the dividend polynomial do **not** enter the remainder, whenever possible. The previous statement admits a rigorous formulation in the unambiguous division case (see sec.2.8), namely,

- Only the first-level (see sec. 3.4) minimal remainders for certain initial spin states (but generally not all of them), if uniquely defined, enter the resulting remainder, which yields the knot invariant.

### 6.1.4 Our program

In this section, we present a straightforward way to calculate the explicit form of the generating function for all the CohFT diagrams. The technique relies on the  $\mathcal{R}$  and  $\mathcal{Q}$ -matrix formalism (described in sec. 2.2), in principle being valid for any knot diagram, with any associated Lie algebra and its representations (see sec. 2.1). Here we study the case of fundamental representation of the  $\mathfrak{su}_N$  algebra, when the answer is expected to reproduce the KhR polynomial. We restrict the set of our knot diagrams to braid closures. More specifically, we consider general two-strand braids and particular cases of three-strand braids. Furthermore

we require all crossings to be of type  $\nearrow$ . An  $\nwarrow$  type crossing gives rise to an extra set of solitons [1], which is beyond the scope of the current paper.

We then apply the minimal positive division technique described in sec. 3 to the resulting generating function.

To determine the ambiguous remainder, we involve the idea of the multilevel division from sec. 3.4. Namely, we write a decomposition of type (3.24), with  $Y$  running over the various distributions of the solitons over the turning points, the expansion term with index  $Y$  generating all possible distributions of the solitons over the crossings in the relevant case.

## 6.2 Division algorithm for a generic two strand knot

### 6.2.1 The CohFT calculus in the two-strand case

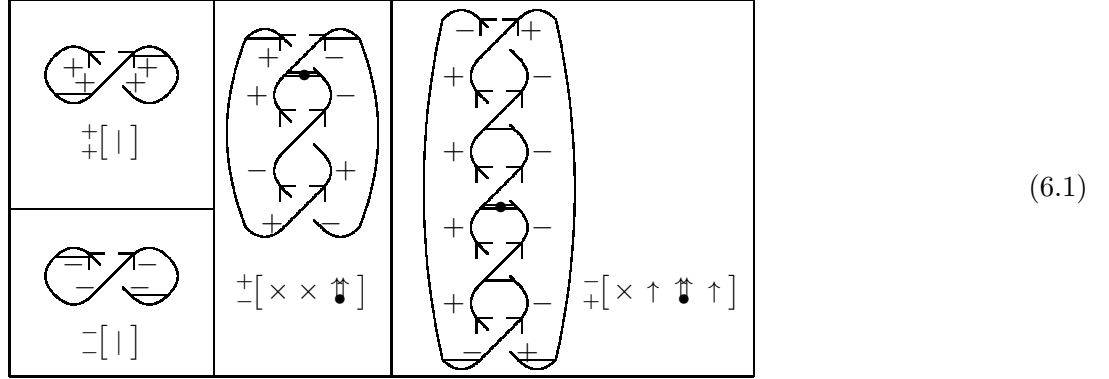
Below we consider a particular case of knot presented as the closure of a two strand positive braid with  $n = 2k + 1$  crossings (all of type  $\nearrow$ ). A two strand braid involving negative crossings are topologically equivalent either to a positive braid or to its reflection depending on whether  $\# \nearrow > \# \nwarrow$  or  $\# \nearrow < \# \nwarrow$  respectively (see App. A.5).

A spin state, + or -, is associated to a strand of the braid. The corresponding label is placed in the picture near each strand segment connecting two crossings. A section of the braid is related then to a composite spin state, ++, +-, -+, or --. The states ++ and -- are conserved throughout the braid, while each of the states +- and -+ can change into one another near crossings. The change happens if a crossing is associated to a soliton. Two kinds of the solitons are drawn on the picture as a single (—) and the double (—●—) lines below the crossings. In addition, one can associate solitons to cups and caps, which close

the braid diagram at the top and the bottom ends. The arrangement of the solitons encodes the initial spin state of the system. All four possible arrangements are illustrated in (6.1), where soliton carrying cups and caps with like  $\cup$  and  $\cap$ , respectively. The obtained picture is called in [1] a *soliton diagram*.

We represent a soliton diagram as a word, where each of  $n$  letters indicates what happens at the corresponding crossing. Namely,  $\times$  stands for the lack of soliton, while  $|$  and  $\updownarrow$  stand for the solitons of the two kinds (following [2], with put the arrows showing the transport of the spin state). We word put the word in the square brackets and write the initial spin states in front of them. The spin states in all other braid sections can be successively obtained as one knows if there is a soliton at each crossing. The final spin state of the system must coincide with the initial one.

The examples of the soliton diagrams together with the corresponding words are given in table (6.1).



Below we enumerate the soliton diagrams with help of the corresponding words, treating the latter ones as products of non-commutative variables (the letters) and construct explicitly the generating function for all the allowed words.

Then we search for an algorithm of presenting the generating function as (3.6)-type decomposition with the desired knot invariant as a remainder. For that we apply the “multi-level” division trick from sec. 3.4 with  $Y \in \{++, --, +-, -+\}$ .

We find that

- The first-level remainders are unambiguous (see sec. 3.2) for any number or crossings.
- The second-level division can be performed algorithmically, by operating with the introduced non-commutative variables according to certain “reduction rules”.

The corresponding “reduction rules” are explicitly formulated below, in ssec. 6.2.2, 6.2.3.

### 6.2.2 Khovanov ( $N = 2$ ) case

1. Calculate

$$\mathfrak{P}^{2,n}(q, T) = \mathfrak{R}_{=}^n \xi_{=} + \text{Tr} \left\{ \mathfrak{R}_{\pm}^n \begin{pmatrix} \xi_{\pm} \\ \xi_{\mp} \end{pmatrix} \right\} \quad (6.2)$$

with

$$\mathfrak{R}_{=} = \begin{pmatrix} q \\ T \end{pmatrix}, \quad \mathfrak{R}_{\pm} = \begin{pmatrix} q & T \\ T & q + Tq^{-1} \end{pmatrix}. \quad (6.3)$$

2. Expand

$$\mathfrak{P}(\xi|q, T) = \sum_Y \mathfrak{P}^Y(q, T) \xi_Y, \quad Y \in \{++, --, +-, -+\}. \quad (6.4)$$

3. Perform the first-level reduction

$$\mathfrak{P}^Y(q, T) = \sum_k q^k \sum_{\vartheta=\vartheta_{Y,k}^{\min}}^{\vartheta=\vartheta_{Y,k}^{\max}} C_{\vartheta,u}^Y T^\vartheta \rightarrow \mathcal{P}_I^Y(q, T) \equiv \sum_k q^k T^{\vartheta_{Y,k}^{\min}}. \quad (6.5)$$

4. Perform the second-level reduction

$$\begin{aligned} 1. \quad & q\xi_+ + q^{-1}T\xi_\pm \rightarrow 0. \\ 2. \quad & T^{2k+1}\xi_\pm + T^{2k+2}\xi_\mp \rightarrow 0. \end{aligned} \quad (6.6)$$

**Do not reduce**  $T^{2k}\xi_\pm + T^{2k+1}\xi_\mp \rightarrow 0$  !

5. Substitute  $\xi_+ = q^2$ ,  $\xi_- = q^{-2}$ ,  $\xi_\pm = \xi_\mp = 1$  .

6. The KhR polynomial equals

$$\boxed{\text{Kh}^{[2,n]}(q, T) = q^{-2n} \mathfrak{P}_I(q, T)}. \quad (6.7)$$

For each particular odd  $n$  the result reproduces the Khovanov polynomial for the two-strand knot with  $n$  crossings (torus knot  $T[2, n]$ ) [7]. The particular case  $n = 5$  is explicitly worked out below. Even  $n$  correspond to links, which we do not consider here.

### 6.2.3 KhR for generic $N$

1. Take the expansion (6.4), reduced as in item 2 of sec. 6.2.2,

$$\mathfrak{P}_I(q, T) = \sum_Y \mathfrak{P}_I^Y(q, T) \xi_Y = \sum_Y \xi_Y \sum_k q^k T^{\vartheta_{Y,k}^{\min}}. \quad (6.8)$$

2. Substitute whenever possible

$$\begin{aligned} 1. \quad & q^n \xi_- + q^{n-2} T \xi_{<} \rightarrow q^{N+n-1} [N]. \\ 2. \quad & q^2 T^{2k+1} \xi_{<} + q^{-2} T^{2k+2} \xi_{>} \rightarrow T^{2k+1} (q^N + T q^{-N}) [N-1]. \end{aligned} \quad (6.9)$$

3. The KhR polynomial of the torus knot  $T[2, n]$  equals

$$\boxed{\text{KhR}_N^{[2,n]}(q, T) = q^{-nN} \mathfrak{P}_I(N|q, T)}. \quad (6.10)$$

The result coincides with formula (4.55) from [3] (earlier proposed in [24] for the superpolynomials).

$$\text{KhR}_N^{[2,n]}(q, T) = q^{-(n-1)(N-1)} \left( [N] + [N-1] (1 + q^{-2}T) \sum_{j=0}^{2j \leq n} q^{n-2j-4} T^{2j} \right). \quad (6.11)$$

### 6.2.4 Primary polynomials as “deformed” HOMFLY polynomials

Expression (6.2) is the result of deformation (2.23) of the  $\mathcal{R}$ -matrix representation for the HOMFLY invariant (2.4), applied to the particular case of a two-strand braid closure [36, 3]. Namely,

$$\mathfrak{P}^{[2,n]} = \mathcal{Q}_{i_1}^{i_{n+1}} \mathcal{Q}_{j_1}^{j_{n+1}} \prod_{k=1}^n \mathfrak{R}_{j_{k+1} i_{k+1}}^{i_k j_k} = \sum_{i=1}^N (\mathcal{Q}_i^i \mathcal{Q}_i^i \mathcal{R}_{ii}^{ii})^n + \sum_{i < j=1}^N \left( \mathcal{Q}_i^i \mathcal{Q}_j^j (\mathfrak{R}_\pm^N)_{ij}^{ij} + \mathcal{Q}_j^j \mathcal{Q}_i^i (\mathfrak{R}_\pm^N)_{ji}^{ji} \right), \quad (6.12)$$

where

$$\mathfrak{R}_= = \mathfrak{R}_{ii}^{ii} = \frac{ii}{q} \left| \begin{array}{c} ii \\ ii \end{array} \right|, \quad 1 \leq i \leq N, \quad \mathfrak{R}_{\pm} = \begin{pmatrix} \mathfrak{R}_{ij}^{ij} & \mathfrak{R}_{ij}^{ji} \\ \mathfrak{R}_{ji}^{ij} & \mathfrak{R}_{ji}^{ji} \end{pmatrix} \cong \begin{array}{c|c} \begin{array}{cc} ij & ji \\ 0 & T \\ T & q + Tq^{-1} \end{array} & \begin{array}{c} ij \\ ji \end{array} \end{array}, \quad 1 \leq i < j \leq N. \quad (6.13)$$

Note that  $\mathfrak{R}_{\pm}$  is obtained from the block of the “deformed”  $\mathcal{R}$ -matrices (2.11) by cancelling the  $q(1+T)$  entry. Since the blocks (6.13) of the  $\mathfrak{R}$ -matrix are independent of  $i$  and  $j$ ,  $\mathcal{Q}$  enters (6.12) only in combinations

$$\xi_= = \sum_{i=1}^N (Q_i^i)^2, \quad \xi_{\pm} = \sum_{i < j=1}^N Q_i^i Q_j^j, \quad \xi_{\mp} = \sum_{j < i=1}^N Q_j^j Q_i^i. \quad (6.14)$$

If one considers  $Q_i^i$  as (generically non-commutative) operators, this yields (6.2). All the  $\xi$ 's must then be treated as formal operators, independent of each other, as well as of  $q$  and  $T$ , until all the reduction steps are performed.

The factors in (6.7, 6.10) are the particular cases of the framing factors (skipped in (2.4), but now restored; see App. A.3, where we should set  $w = n$ , and  $N = 2$  to get (6.10)).

The substitutions in item 2 of sec. 6.2.3 are motivated by the identities for the corresponding terms in the HOMFLY polynomial, respectively,

$$q\xi_+ + q^{-1}T\xi_< \xrightarrow{\text{HOMFLY}} q \frac{[2N]}{[2]} - q^{-1} \frac{[N][N-1]}{[2]} = q[N]^2 - [N][N-1] = q^N[N] \\ \parallel \\ [N]^2 - \frac{[N][N-1]}{[2]}, \quad (6.15)$$

and

$$q^2\xi_> + q^{-2}T\xi_< \xrightarrow{\text{HOMFLY}} (q^2 - q^{-2}) \frac{[N][N-1]}{[2]} = (q - q^{-1})[N][N-1] = (q^N - q^{-N})[N-1]. \quad (6.16)$$

### 6.2.5 Comparing the $N = 2$ and $N > 2$ cases

**The reduction rules:  $N = 2$  as a particular case of generic  $N$ .** The level II reduction rules look differently for  $N = 2$  (sec. 6.2.2, item 4) and for generic  $N$  (sec. 6.2.3, item 2). Here we comment on their relationship.

The first of the  $N = 2$  rules, written in schematic form

$$q^n \xi_+ + q^{n-2} T \xi_{\pm} \rightarrow q^{n-1} [2], \quad (6.17)$$

with  $\xi_+ \equiv \xi_+ + \xi_-$ , just takes the form of the general rule, with  $N = 2$  substituted.

The case of the second rule is different. Namely, the  $N = 2$  rule (item 4 from sec. 6.2.2) is manifestly asymmetric between the odd and even  $T$  powers (see the comment in the boldface), while the general  $N$  rule (item 3 from sec.6.2.3) appear to be symmetric. In fact, there are several versions of the reduction rule for  $N \geq 3$ , all yielding the same remainder. In particular, one can take a straightforward generalization of the  $N = 2$  rule, which is illustrated in Tab. 6.18, 6.19.II for the  $N = 2$  and  $N = 3$  cases. One should compare this with the rule in Tab. 6.19.I, which we adhere to, and one more possibility in Tab. 6.19.III.

$$\begin{array}{|c|c|} \hline N = 2 & \min(i, j) \\ \hline \max(i, j) & 0 \\ \hline 1 & q \cdot q^{-1} \\ \hline \end{array} \times \begin{array}{|c|c|c|c|} \hline \begin{array}{c} \cancel{q^2} \\ q^3 T^2 \end{array} & \begin{array}{c} q^{-1} T^3 \\ \cancel{q^3} \end{array} & \begin{array}{c} \cancel{q^{-3} T^4} \\ q^{-1} T^4 \end{array} & \begin{array}{c} q^{-5} T^5 \\ \cancel{q^{-3} T^5} \end{array} \\ \hline \end{array} \begin{array}{l} q^{-1} T^3 + q^{-1} T^4 \not\rightarrow 0; \\ q T^2 + q T^3 \rightarrow 0, \quad q^{-1} T^4 + q^{-3} T^5 \rightarrow 0. \end{array} \begin{array}{l} i < j \\ i > j \end{array} \quad (6.18)$$

$N = 3$	$\min(i, j)$
$\max(i, j)$	1    0
2	$q^2 \cdot 1$ $q^2 \cdot q^{-2}$
1	1 $q^{-2}$

 $\times$ 

$qT^2$	$q^{-1}T^3$	$i < j$
$q^3T^2$	$qT^3$	$i > j$

I

$q[2]T^2 (q + q^{-1}T) [3] \rightarrow qT^2[2] (q[2](q^3 + q^{-3}T))$	
$qT^2 \times \begin{pmatrix} \boxed{q^2} & \nearrow X \\ & \searrow q^{-2} \end{pmatrix}$	$q^{-1}T^3 \times \begin{pmatrix} \nearrow q^2 & \nearrow X \\ & \boxed{q^{-2}} \end{pmatrix}$
$q^3T^2 \times \begin{pmatrix} \boxed{q^2} & \searrow q^{-2} \\ & \searrow q^{-2} \end{pmatrix}$	$qT^3 \times \begin{pmatrix} \searrow q^2 & \searrow X \\ & \boxed{q^{-2}} \end{pmatrix}$

(6.19)

II

 $q^2T^2(q + q^{-1}T)[3] \rightarrow qT^2(q^2 + q^{-2}T)[2]$ 
 $qT^2(1 + T)[3] \rightarrow 0$ 

$qT^2 \times \begin{pmatrix} q^2 & 1 \\ & q^{-2} \end{pmatrix}$	$q^{-1}T^3 \times \begin{pmatrix} \searrow q^2 & \boxed{1} \\ & \boxed{q^{-2}} \end{pmatrix}$
$q^3T^2 \times \begin{pmatrix} \boxed{q^2} & \boxed{1} \\ & \searrow q^{-2} \end{pmatrix}$	$qT^3 \times \begin{pmatrix} q^2 & 1 \\ & q^{-2} \end{pmatrix}$

III

$qT^2 \times \begin{pmatrix} \searrow q^2 & \nearrow X \\ & \searrow q^{-2} \end{pmatrix}$	$q^{-1}T^3 \times \begin{pmatrix} \nearrow q^2 & \boxed{1} \\ & \boxed{q^{-2}} \end{pmatrix}$
$q^3T^2 \times \begin{pmatrix} \boxed{q^2} & \boxed{1} \\ & \searrow q^{-2} \end{pmatrix}$	$qT^3 \times \begin{pmatrix} \searrow q^2 & \nearrow X \\ & \searrow q^{-2} \end{pmatrix}$

In particular, one can see from the tables (6.19) that the odd-even asymmetry in fact is present in all versions of the reduction rules. However, the resulting remainder does not include a  $\sim (1 + T)$  contribution in case  $N \geq 3$ . The difference is due to the additional  $q$ -power factors (arranged below in the triangle matrices), which account for various initial states giving rise to the same set of the soliton diagrams. Hence,

- The KhR polynomial of a two-strand knot is a minimal remainder for  $N \geq 3$ , unlike the Khovanov polynomial ( $N = 2$ ) of the same knot.

To summarize,

- The  $N = 2$  reduction rules are a particular case of the generic  $N$  reduction rules,

in the considered case of the two-strand knots. However, **this is not so for a general knot** because naive substitution of  $N = 2$  in the (large  $N$ ) KhR polynomial does not always yield the correct Khovanov polynomial (compare the explicit examples in [22] with that in [7], and see e.g., in [3] for discussion).

Now we return to the  $N = 2$  (Khvanov) case, which provides enough illustrations to the following discussion.

### 6.2.6 The primary polynomial as the generating function for the soliton diagrams

Diagram rules (A.33) from [1] can be written in the matrix notations as

$$\mathfrak{B} \rightarrow \hat{\mathfrak{B}} : \quad \mathfrak{R}_\pm \rightarrow \hat{\mathfrak{R}}_\pm = \begin{pmatrix} | & \end{pmatrix}, \quad \mathfrak{R}_\pm \rightarrow \hat{\mathfrak{R}}_\pm = \begin{pmatrix} 0 & \times & \uparrow \\ \times & \uparrow & \times \\ \times & \uparrow & \uparrow \end{pmatrix}, \quad (6.20)$$

(one must substitute  $q \rightarrow qT$ ,  $[0] \rightarrow 1$ ,  $[f_0] \rightarrow 1$ ,  $[f_0 + 1] \rightarrow T$  in (A.33) and extract the common factor  $q^{-\frac{1}{2}}$  to obtain our formulas). The primary polynomial (6.2) subjected to further “deformation” (6.20) thus becomes the generating function for the soliton diagrams from [1]. If we put  $N = 2$  and  $i, j \in \{+, -\}$  in (6.12) (a more detailed version of (6.2)), then the upper and the lower pair of indices of each  $\mathfrak{R}$  corresponds to the composite spin state below and above the corresponding crossing, respectively. The braids with the composite spin state  $++$  and  $--$  in the first (and hence in any other) section are enumerated by the diagonal terms entering with the coefficient  $\xi_\pm$ , and all such diagrams yield the same “amplitude”  $\mathfrak{R}_\pm^n$ . In turn, the braids with composite spin states  $+-$  or  $-+$  in each section are enumerated by the off-diagonal terms. These states can exchange in each crossing in the way encoded in the 2 matrix  $\hat{\mathfrak{R}}_\pm$  in (6.20), so that all possible soliton diagrams are enumerated by the expansion of the trace in (6.2), where the diagram with the initial spin state  $+-$  or  $-+$  enters with the coefficient  $\xi_\pm$  or  $\xi_\mp$ , respectively.

**Combinatorial expressions for the numbers of the soliton diagrams.** The number of the soliton diagrams with initial spin state  $\pm$  or  $\mp$  can as well be explicitly computed from combinatorial considerations, respectively,

$$\# \left\{ \begin{array}{l} + \\ - \end{array} \left[ \left( \times \times^c \uparrow^w \updownarrow^b \right) \right] \right\} = \frac{(w+b+c)!}{w!b!c!}, \quad w+b+2c=n, \quad (6.21)$$

and

$$\# \left\{ \begin{array}{l} - \\ + \end{array} \left[ \times \left( \times \times^c \uparrow^w \updownarrow^b \right) \times \right] \right\} = \frac{(w+b+c)!}{w!b!c!}, \quad w+b+2c=n-2, \quad (6.22)$$

where the notations in the l.h.s. imply that we count distinct configurations obtained by the various permutations of  $w$  letters  $|$ ,  $b$  letters  $\updownarrow$ , and  $c$  letters  $\times$  in the parentheses. Denied that numbers (6.21) and (6.22) are polynomial coefficients in the expansion of  $(x+y+z)^{w+b+c}$ , the proper generating functions

$$\begin{aligned} f_n^\pm(x, y, z) &= \sum_{w+b+2c=n} \frac{(w+b+c)!}{w!b!c!} x^w y^b z^{2c} = \Phi_{1,1}^n, \\ f_n^\mp(x, y, z) &= f_{n-2}^\pm(x, y, z) = \Phi_{2,2}^n, \end{aligned} \quad (6.23)$$

are expressed for generic  $n$  either as elements of powers of the matrix

$$\Phi = \begin{pmatrix} 0 & c \\ c & w+b \end{pmatrix}, \quad (6.24)$$

or as rational functions of its eigenvalues

$$\lambda_{1,2} = \frac{1}{2} \left( w+b \pm \sqrt{(b+w)^2 + 4c^2} \right). \quad (6.25)$$

These functions becomes the polynomials only if one substitutes the particular integer for  $n$ .

For the initial spin states  $--$  and  $++$  one gets trivially

$$\# \left\{ \begin{array}{l} + \\ + \end{array} \left[ \left( |^n \right) \right] \right\} = \# \left\{ \begin{array}{l} - \\ - \end{array} \left[ \left( |^n \right) \right] \right\} = 1 \quad (6.26)$$

with the generating function  $f_n^-(x) = 2x^n$ .

$$(6.27)$$

Primary polynomial (6.2, 6.3) is then obtained from the entire generating function

$$f^n(x, y, z) = \xi_- f_-^n(x, y, z) + \xi_\pm f_\pm^n(x, y, z) + \xi_{mp} f_\mp^n(x, y, z) \quad (6.28)$$

as the result of the substitution

$$\mathfrak{P}^{2,n}(\xi, q, T) = f^n(q, q^{-1}T, T). \quad (6.29)$$

**Employing the selection rules for the matrix elements in the division procedure.** Deformation rule (6.20) sets a one-to-one correspondence between the monomials in primary polynomial (6.2) and the soliton diagrams. Then,

- The pairs of terms to delete in the reduction rules of sec. 6.2.2 correspond to the pairs of soliton diagrams of [1] between which the transition is allowed<sup>20</sup>.

---

<sup>20</sup>In fact, the allowed transitions in [1] are related to a slightly different reduction rules, yet producing the same answer (see the explicit example below)

**Covariance under cyclic permutations.** The suggested reduction rules are not invariant, but rather covariant under the equivalence transformations of the knot diagram, namely under the cyclic shift of the crossings (this is the only transformation relevant for two-strand braids [6]).

The table below illustrates the behaviour of the various soliton diagrams under the cyclic shift for two-strand braid with  $n = 3$  crossings (the closure is the trefoil knot,  $3_1$  in [7]). Each diagram in the leftmost column is mapped to itself. The diagrams arranged in triangles are mapped into each other along the arrows. The cancellation of the diagrams arranged in the vertical pairs obeys the local rule  $(\uparrow \uparrow) + (\times \times) \sim 0$  (see [1]) for detailed discussion of this rule in particular cases).

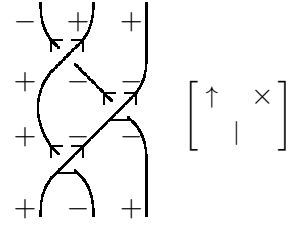
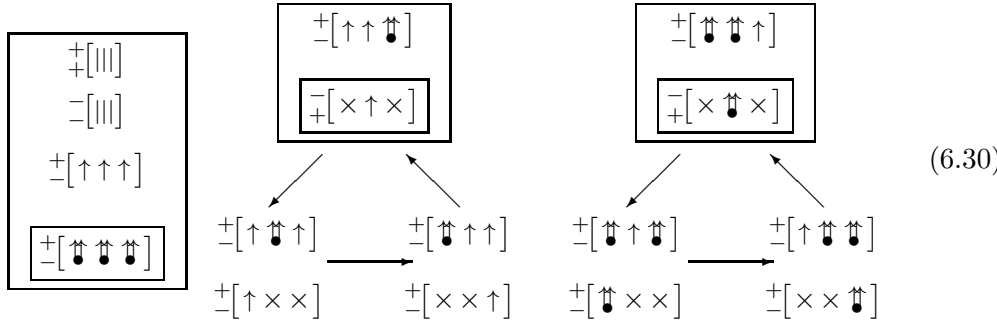


Figure 4: A piece of a three strand braid  $\mathcal{B} = (\dots, 1, 2, 1, \dots)$ , with a possible distribution of the spin states (+ and -) on the stands, and of the solitons in the crossings. On the right is our notation for the obtained diagram.



### 6.2.7 Example: torus knot $T^{2,5}$ .

The simplest example, when all the above features are non-trivial, is presented in Tab. 5. Nothing essentially new happens for a two-strand knot with an arbitrary number of crossings.

The contributions to the first-level remainder are boxed. The contributions to the second-level remainder are double boxed. The terms marked by the same Roman numerals (uppercase) “cancel each other” under the second level reduction. The lowercase labels mark the pairs of terms “cancelling” in the [1] version of the reduction instead. The resulting remainders in the two cases contain different sets of the soliton diagrams but are equal as polynomials in  $q$  and  $T$ , both yielding the correct value of the Khovanov polynomial for  $T[2, 5]$  knot ( $5_1$  in [7]).

## 6.3 The first-level division for particular three-strand knots

Now we turn to the first attempt to treat a more general case using our approach which is the hybrid between the CohFT calculus and positive division technique.

Below we restrict our considerations to the case of Khovanov polynomials ( $N = 2$ ), which already appear to be rather involved.

### 6.3.1 A draft of the three-strand reduction procedure

The list below almost literally follows the two-stand algorithm, yet differing at each step, with the most steps not being completely worked out at the moment.

1. For a three-strand braid  $\mathcal{B} = (\mathcal{B}_i)_{i=1}^n$ ,  $\mathcal{B}_i = 1, 2$  (fig. 4),

$$\mathfrak{P}^{\mathcal{B}}(q, T) = \sum_Y \text{Tr } \mathcal{Q}^Y(q) \prod_{i=1}^n \mathfrak{R}_{\mathcal{B}_i}^Y(q, T), \quad Y \in \{(000), (001), (011), (111)\}. \quad (6.31)$$

with

$$\mathcal{Q}^{(000)} = (\xi_{000}), \quad \mathcal{Q}^{(001)} = \text{diag}(\xi_{001} \xi_{010} \xi_{100}), \quad \mathcal{Q}^{(011)} = \text{diag}(\xi_{011} \xi_{101} \xi_{110}), \quad \mathcal{Q}^{(111)} = (\xi_{111}), \quad (6.32)$$

$$\mathfrak{R}_{-\mathcal{B}_i}^Y(q, T) = \mathfrak{R}_{\mathcal{B}_i}^Y(q^{-1}, T), \quad \text{and } \mathfrak{R}_{\mathcal{B}_i}^Y(q, T) \text{ for } \mathcal{B}_i > 0 \text{ given by (6.36).}$$



Table 5: Torus knot [2, 5]. Soliton diagrams associated with all the terms of the primary polynomial, in the first-level remainders (boxed), and in the Khovanov polynomial (double boxed).

$\mp$	$[5   ]$ $\boxed{q^5}$ <b>1</b>					
$=$	$[5   ]$ $\boxed{q^5}$ <b>1</b> I, <i>i</i>					
$\pm$	$[(5 \uparrow)]$ <b>1</b> $\boxed{q^5}$ $\parallel$ $q^5$	$[(\uparrow 4 \uparrow)]$ <b>5</b> = $\frac{5!}{1!4!}$ $\boxed{q^3 T}$ $\parallel$ $q^4 (q^{-1}T)$ I, <i>i</i>	$[(2 \uparrow 3 \uparrow)]$ <b>10</b> = $\frac{5!}{2!3!}$ $\boxed{qT^2}$ $\parallel$ $q^3 (q^{-1}T)^2 =$ II	$[(3 \uparrow 2 \uparrow)]$ <b>10</b> $\boxed{q^{-1}T^3}$ $\parallel$ $q^2 (q^{-1}T)^5$ <i>ii</i>	$[(\uparrow 4 \uparrow)]$ <b>5</b> $\boxed{q^{-3}T^4}$ $\parallel$ $q (q^{-1}T)^4$ III	$[(5 \uparrow)]$ <b>1</b> $\boxed{q^{-5}T^5}$ $\parallel$ $(q^{-1}T)^5$ <i>iii</i>
		$[(3 \uparrow \times \times)]$ <b>4</b> $q^3 T^2$ $\parallel$ $q^3 \cdot T^2$	$[(2 \uparrow \uparrow \times \times)]$ <b>12</b> = $\frac{3! (3+1)!}{1!2! 3!1!}$ $qT^3$ $\parallel$ $q^2 (q^{-1}T) \cdot T^2$	$[(\uparrow 2 \uparrow \times \times)]$ <b>12</b> $q^{-1}T^4$ $\parallel$ $q (q^{-1}T)^2 \cdot T^2$	$[(3 \uparrow \times \times)]$ <b>4</b> $q^{-3}T^5$ $\parallel$ $(q^{-1}T)^3 \cdot T^2$	
			$[(\uparrow 2 \times \times)]$ <b>3</b> = $\frac{(2+1)!}{2!1!}$ $\star qT^4$ $\parallel$ $q \cdot T^2 \cdot T^2$	$[(\uparrow 2 \times \times)]$ <b>3</b> $\star q^{-1}T^5$ $\parallel$ $(q^{-1}T) \cdot T^2 \cdot T^2$		
$\mp$		$[\times (3 \uparrow) \times]$ <b>1</b> $\boxed{q^3 T^2}$ $\parallel$ $T \cdot q^3 \cdot T$ <i>ii</i>	$[\times (2 \uparrow \uparrow) \times]$ <b>3</b> = $\frac{3!}{1!2!}$ $\boxed{qT^3}$ $\parallel$ $T \cdot q^2 (q^{-1}T) \cdot T$ II	$[\times (\uparrow 2 \uparrow) \times]$ <b>3</b> $\boxed{q^{-1}T^4}$ $\parallel$ $T \cdot q (q^{-1}T)^2 \cdot T$ <i>iii</i>	$[\times (3 \uparrow) \times]$ <b>1</b> $\boxed{q^{-3}T^5}$ $\parallel$ $T \cdot (q^{-1}T)^3 \cdot T$ III	
			$[\times (\uparrow) \times \times \times]$ <b>2</b> $qT^4$ $\parallel$ $T \cdot q \cdot T^2 \cdot T$	$[\times (\uparrow \times \times) \times]$ <b>2</b> $q^{-1}T^5$ $\parallel$ $T \cdot (q^{-1}T) \cdot T^2 \cdot T$		

2. Expand

$$\mathfrak{P}(\xi|q, T) = \sum_Y \mathfrak{P}^Y(q, T) \xi_Y, \quad Y \in \{(000), (001), (011), (111)\}. \quad (6.33)$$

3. I. Reduce

$$\mathfrak{P}^Y(q, T) = (1 + T)\mathcal{J}^Y(q, T) + \mathcal{P}_{\min}^Y(q, T) \rightarrow \mathcal{P}_{\min}^Y(q, T), \quad (6.34)$$

to the residue containing the minimal possible number of  $q$  and  $T$  powers, **if it is unique**.

4. II. Reduce further

$$\sum \mathcal{Q}^Y \mathcal{P}_{\min}^Y(q, T) \rightarrow ? \quad (6.35)$$

5. Substitute  $\xi_{000} = q^3$ ,  $\xi_{001} = \xi_{010} = \xi_{100} = q$ ,  $\xi_{011} = \xi_{101} = \xi_{110} = q^{-1}$ ,  $\xi_{111} = q^{-3}$ .

6. The result must be proportional to the Khovanov polynomial of the knot  $\mathcal{K} = \overline{\mathcal{B}}$  that is the closure of the braid  $\mathcal{B}$  (the proportionality factor is  $q^{-2w}$  with  $w = \sum_{i=1}^N \mathcal{B}_i$ , see sec. 6.2.4).

### 6.3.2 Explicit formulas for the three-strand (deformed) $\mathcal{R}$ -matrices

From now on we switch to the notations  $+ \rightarrow 0$  and  $- \rightarrow 1$ , more natural for the  $\mathcal{R}$ -matrix formalism (especially when aiming for the general  $N$  case). Just as in the two-strand case, we omit all the  $q(1 + T)$  entries in the  $\mathcal{R}$ -matrices (as the sources of  $\sim (1 + T)$  contributions never enter the minimal remainders). All the needed matrices are explicitly given in the table below.

To compute		<b>I</b>	<b>II</b>	<b>III</b>	
$Y$	$k$	HOMFLY polynomial	Primary polynomial	Generating function	
		$\mathcal{R}_k^Y$	$\mathfrak{R}_k^Y$	$\hat{\mathfrak{R}}_k^Y$	
(000), (111)	1, 2	$\frac{iii}{(q)} \Big  iii, i = 0, 1$	$(q)$	$(   )$	
(001)	1	$\frac{001 \quad 010 \quad 100}{\left( \begin{array}{ccc c} q & & & 001 \\ & q - q^{-1} & -1 & 010 \\ & -1 & & 100 \end{array} \right)}$	$\left( \begin{array}{ccc} q & & \\ & q + q^{-1}T & T \\ & T & \end{array} \right)$	$\left( \begin{array}{ccc c}   & & & \times \\ & \uparrow + \updownarrow & & \\ & \times & & \end{array} \right)$	
	2	$\frac{001 \quad 010 \quad 100}{\left( \begin{array}{ccc c} q - q^{-1} & -1 & & 001 \\ -1 & & & 010 \\ & & q & 100 \end{array} \right)}$	$\left( \begin{array}{ccc} q + q^{-1}T & T & \\ T & & q \end{array} \right)$	$\left( \begin{array}{ccc c}   + \updownarrow & & \times & \\ & \times & & \\ & & &   \end{array} \right)$	(6.36)
(011)	1	$\frac{011 \quad 101 \quad 110}{\left( \begin{array}{ccc c} q - q^{-1} & -1 & & 101 \\ -1 & & & 101 \\ & & q & 110 \end{array} \right)}$	$\left( \begin{array}{ccc} q + q^{-1}T & T & \\ T & & q \end{array} \right)$	$\left( \begin{array}{ccc c}   + \updownarrow & & \times & \\ & \times & & \\ & & &   \end{array} \right)$	
	2	$\frac{011 \quad 101 \quad 110}{\left( \begin{array}{ccc c} q & & & 011 \\ & q - q^{-1} & -1 & 101 \\ & -1 & & 110 \end{array} \right)}$	$\left( \begin{array}{ccc} q & & \\ & q + q^{-1}T & T \\ & T & \end{array} \right)$	$\left( \begin{array}{ccc c}   & & & \times \\ &   + \updownarrow & & \\ & \times & & \end{array} \right)$	

## 6.4 The generating function for the three-strand soliton diagrams

Similarly to the two-strand case, expression (6.31) for the three-strand primary polynomial turns into a generating function for the soliton diagrams associated with the braid  $\mathcal{B}$ , if one substitutes  $\hat{\mathfrak{R}}$  from col. **III** instead of  $\mathfrak{R}$  from from col. **II** of (6.36), each monomial in the primary polynomial being then related to a certain soliton diagram.

We consider only the positive braids, i.e., all the crossings being the  $\nearrow$  type, and respectively all  $\mathcal{B}_i > 0$ . The form of a three strand braid is much more constrained by such assumption, than the form of a two strand braid (see sec. 6.2).

### 6.4.1 Guide to the experimental data

The three-strand positive braids with no more than 8 crossings, together with the knots or links being their closures, are enumerated in App. D. Examples of the unique remainders, with each term related to a set of soliton diagrams, are given in App. E:

1. for the doubly twisted unknot diagram, presented as three-strand braid with 2 crossings (App. E.1),
2. for all possible diagrams of the trefoil knot having form of three-strand braids with 4 crossings and providing the unique first level remainders (App. E.2)
3. for torus knot  $T[3, 4]$  ( $8_{19}$  in [7]), presented as a three-strand braid with 8 crossings <sup>21</sup>.

## 7 Further directions

We complete our presentation by enumerating the most natural directions for the following research.

1. **Systematic study of the  $m \geq 3$  strand case.** Of course, the attempt presented in sec. 6.3 is just the first and a very naive one.
2. **Relation to the standard Khovanov-Rozansky construction.** It is mysterious that the KhR construction, apparently following just one of several possible options at many points of the procedure (in particular, see the footnotes in the beginning of sec. 2.4 and in the beginning of 2.6), is discussed in the mathematical literature only in its original literal formulation [4, 22] ???  $N = 3$  ??? . Any alternative (even not essentially different mathematically), if found, can be useful for various applications. A detailed comparison of the  $\mathcal{R}$ -matrix construction, schematically described in sec. 2 and in sec. 4, with the rigorously formulated KhR construction, both on the general level and with explicit examples, provides some advances in this direction.
3. **Relation to the differential expansion.** This issue touched in sec. 5 definitely deserves a systematic treatment.
4. **The problem of finite  $N$ .** The problem is in particular discussed in [3] and mentioned in sec. 6.2.5. The definition of the KhR polynomial [4] initially refers to the same notions, as the  $\mathcal{R}$ -matrix definition of the HOMFLY polynomial, until the differentials are introduced. In particular, both invariants are associated with the  $\mathfrak{su}_N$  series of the Lie algebras (we tried to present this point mostly explicit in sec. 2). However, the HOMFLY invariants admit the most naive analytical continuation to arbitrary complex value of  $N$ , while the KhR polynomials admits one only for  $N \leq N_0$  (with  $N_0$  depending on the knot). The “phase transition” at  $N = N_0$ , which definitely happens at the level of homologies, is still not well studied and attracts a lot of attention.

---

<sup>21</sup>This case deserves special interest, as the simplest case of the “thick” knot, i.e., when the Khovanov polynomial is **not** recovered by setting  $N = 2$  in the KhR polynomial [3].

5. **Higher representations and other groups.** Finally, the  $\mathcal{R}$ -matrix based approach possesses a highly inspiring property, already mentioned in sec. 2. Namely, in principle it can be extended to *arbitrary* Lie groups and representations, on the ground of the already existing  $\mathcal{R}$ -matrix approaches to other knot invariants [6]. The coloured (related to higher representations of the  $\mathfrak{su}_N$  Lie algebra) analogs of the KhR invariants are widely studied in various (often semi-empiric) ways [24, 25, 27, 28, 31, 9] (the list of references can be expanded). Yet the subject is even further from being exhausted, than the case of ordinary KhR invariants. In particular, even exact definition of the coloured KhR invariants (superpolynomials) faces essential difficulties, in particular, discussed in [30, 32] (the second paper concerns a possible extension of the cabling approach [44] to the superpolynomials).
6. **Can one use the CohFT calculus as a tool in the KhR calculus?** This is the most intriguing point of the story. In fact, this work was originally motivated by this question. Authors of [1, 2] follow the CohFT logic and associate the knot polynomials with the partition function for BPS states. They consider the resolutions of the knot diagram (representing the basis vectors in the complex) as the soliton states in the CohFT, and they relate the action of the differentials to the instantons responsible for the soliton scattering. They also discuss the wall-crossing phenomenon in this context. Yet, all their considerations remain rather a matter of art, than a regular technique. It is still unclear, whether the such technique can at all be developed in the CohFT framework.

## Acknowledgements

The author is deeply indebted to A. Yu. Morozov for scientific direction of this work, and to D. Galakhov and I. Danilenko for long inspiring discussions and patient explanations. The author truly appreciates the great work of Ye. Zenkevich, who carefully read the draft and helped to prepare it for publishing, and also the work of G. Aminov, who helped to correct the appendices. The author thanks S. Arthamonov, And. Morozov and A. Popolitov for the valuable comments, and M. Bishler, D. Vasiliev, Ya. Kononov, S. Mironov, N. Nemkov, A. Sleptsov together with all other participants of the Mathematical physics group seminar for interest to this work.

The author is also grateful to the secretary of the mathematical physics group E. S. Syslova, who makes the work of the author and his colleagues possible for many years.

This work was funded by the Russian Science Foundation (grant N 16-12-10344).

## References

- [1] Galakhov D., Moore G. — arXiv : hep-th/1607.04222.
- [2] Galakhov D. — arXiv : hep-th/1702.07086.
- [3] Anokhina A., Morozov A. // JHEP. — 2014. — Vol. 07, no. 063. — arXiv : hep-th/1403.8087.
- [4] Khovanov M., Rozansky L. Matrix factorizations and link homology // Fund. Math. — 2008. — Vol. 199. — P. 1–91. — arXiv : math.QA/0401268.
- [5] Khovanov M. A categorification of the Jones polynomial // Duke Math. J. — 2000. — Vol. 101. — P. 359–426.
- [6] Kauffman L. H. The interface of knots and physics. — Singapore : World Scientific, 2001. — P. 788.
- [7] Bar-Natan D., Scott M., et al. The Knot Atlas. — URL: <http://katlas.org> (online; accessed: 22.10.17).
- [8] Morozov And., Sleptsov A., et al. The knotbook. — URL: [www.knotbook.org](http://www.knotbook.org) (online; accessed: 22.10.17).

- [9] Gukov Sergei, Khovanov Mikhail, Walcher Johannes. *Physics and Mathematics of Link Homology*. — Providence : AMS, 2016. — P. 177.
- [10] Gukov S., Schwarz A., Vafa C. Khovanov-Rozansky homology and topological strings // *Lett. Math. Phys.* — 2005. — Vol. 74. — P. 53–74. — arXiv : hep-th/0412243.
- [11] Rasmussen Jacob. — 2006. — arXiv : math.GT/0607544.
- [12] Dunfield N. M., Gukov S., Rasmussen J. The superpolynomial for knot homologies // *Experimental Math.* — 2006. — Vol. 15. — P. 129–159. — arXiv : math/0505662.
- [13] Gorsky Eugene, Lewark Lukas // *Experimental Mathematics*. — 2015. — Vol. 24. — P. 162–174. — arXiv : math.GT/1404.0623.
- [14] Gaiotto D., Witten E. — arXiv : hep-th/1106.4789.
- [15] Schwarz A. S. New topological invariants arising in the theory of quantized fields // *International Topological Conference*. — Vol. 2. — Baku : Institute of Mathematics and Mechanics of the Azerbaijan Academy of Sciences of USSR, 1987.
- [16] Witten E. Quantum field theory and the Jones polynomial // *Comm. Math. Phys.* — 1989. — Vol. 121. — P. 351–399.
- [17] Witten E. Gauge theories and integrable lattice models // *Nucl. Phys.* — 1989. — Vol. B322. — P. 629–697.
- [18] Bar-Natan D. On Khovanov’s categorification of the Jones polynomial // *Algebr. Geom. Topol.* — 2002. — Vol. 2. — P. 337–370. — arXiv : math.QA/0201043.
- [19] Dolotin V., Morozov A. Introduction to Khovanov homologies. I. Unreduced Jones superpolynomial // *JHEP*. — 2013. — Vol. 1301, no. 065. — arXiv : hep-th/1208.4994.
- [20] Dolotin V., Morozov A. Introduction to Khovanov homologies. II. Reduced Jones superpolynomials // *J. Phys.: Conf. Ser.* — 2013. — Vol. 411, no. 012013. — arXiv : hep-th/1209.5109.
- [21] Nawata Satoshi, Oblomkov Alexei. *Proceedings of*.
- [22] Carqueville N., Murfet D. Computing Khovanov-Rozansky homology and defect fusion // *Algebr. Geom. Topol.* — 2014. — Vol. 14. — P. 489–537. — arXiv : hep-th/1108.1081.
- [23] Dolotin V., Morozov A. Introduction to Khovanov homologies. III. A new and simple tensor-algebra construction of khovanov-rozansky invariants // *Nucl. Phys.* — 2014. — Vol. B878. — P. 12–81. — arXiv : hep-th/1308.5759.
- [24] Superpolynomials for torus knots from evolution induced by cut-and-join operators / P. Dunin-Barkowski, A. Mironov, A. Morozov et al. // *JHEP*. — 2013. — Vol. 03, no. 021. — arXiv : hep-th/1106.4305.
- [25] Mironov A., Morozov A., Morozov An. Evolution method and “differential hierarchy” of colored knot polynomials // *AIP Conf. Proc.* — 2013. — Vol. 1562. — arXiv : hep-th/1306.3197.
- [26] Evolution method and HOMFLY polynomials for virtual knots / L. Bishler, A. Morozov, And. Morozov, Ant. Morozov // *Int. J. of Mod. Phys.* — 2015. — Vol. A30, no. 1550074. — arXiv : hep-th/1411.2569.
- [27] Gorsky E., Gukov S., Stosic M. Quadruply-graded colored homology of knots. — 2014. — arXiv : math.QA/1304.3481.
- [28] S.Arthamonov, A.Mironov, A.Morozov // *Theor.Math.Phys.* — 2014. — Vol. 179. — P. 509–542. — arXiv : hep-th/1306.5682.

- [29] Kononov Ya., Morozov A. // JETP Letters. — 2015. — Vol. 101. — P. 831–834. — arXiv : hep-th/1504.07146.
- [30] Khovanov Mikhail // Knot theory and its Ramifications. — 2005. — Vol. 14, no. 1. — P. 111–130. — arXiv : math.QA/0302060.
- [31] Nawata S., Ramadevi P., Zodinmawia // JHEP. — 2014. — Vol. 1401, no. 126. — arXiv : hep-th/1310.2240.
- [32] Danilenko I. — arXiv : hep-th/1405.0884.
- [33] Turaev V. G. The Yang-Baxter equation and invariants of links // Invent. Math. — 1988. — Vol. 92. — P. 527–533.
- [34] Reshetikhin N. Yu., Turaev V. G. Ribbon graphs and their invariants derived from quantum groups // Commun. Math. Phys. — 1990. — Vol. 127. — P. 1–26.
- [35] Morozov A., Smirnov A. Chern-simons theory in the temporal gauge and knot invariants through the universal quantum R-matrix // Nucl. Phys. — 2010. — Vol. B835. — P. 284–313. — arXiv : hep-th/1001.2003.
- [36] Mironov A., Morozov A., Morozov And. Character expansion for HOMFLY polynomials. II. fundamental representation. up to five strands in braid // JHEP. — 2012. — Vol. 03. — arXiv : hep-th/1112.2654.
- [37] Anokhina A. On R-matrix approaches to knot invariants. — 2014. — arXiv : hep-th/1412.8444v2.
- [38] Klimyk A., Schmüdgen K. Quantum groups and their representations. — Berlin : Springer, 2012. — P. 552.
- [39] Groups Loop. Andrew Pressley and Graeme Segal. — Oxford : Clarendon Press, Oxford Mathematical Monographs, 1988. — P. 316.
- [40] S.I. Gelfand, Yu.I. Manin. Homological Algebra. — Berlin : Springer, 1994. — P. 222.
- [41] G.Fourier, P.Littellmann // Advances in Mathematics. — 2007. — Vol. 211, no. 2. — P. 566–593. — arXiv : hep-th/1702.07086.
- [42] Elias Ben, Hogancamp Matthew. — 2016. — arXiv : math.GT/1603.00407.
- [43] Hogancamp Matthew. — 2017. — arXiv : math.GT/1704.01562.
- [44] A.Anokhina, An.Morozov // Theor.Math.Phys. — 2014. — Vol. 178. — P. 1–58. — arXiv : hep-th/1307.2216.
- [45] Sergei Gukov Marko Stosic // Geometry & Topology Monographs. — 2012. — Vol. 18. — P. 309–367. — arXiv : hep-th/1112.0030.

## A Basic properties of the special point operators

### A.1 General constraints on the special point operators

#### A.1.1 Continuous space transformations and transformations of the knot diagram.

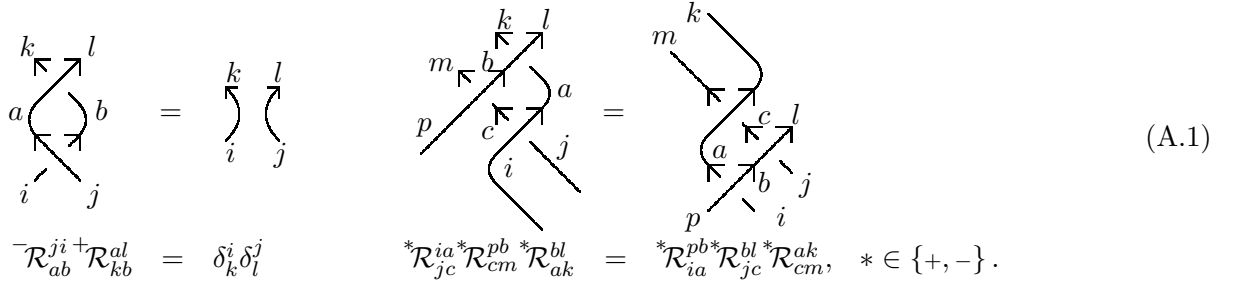
The knot  $\mathcal{K}$  as a curve in the space is considered up to arbitrary continuous space transformations. However, the corresponding transformations of the knot diagram  $\mathcal{D}(\mathcal{K})$  (see sec. 2) include, apart from arbitrary continuous plane transformations, certain singular transformations generated by the *Reidemeister moves* [6]. The latter ones are the elementary transformations of the special points on the knot diagram. Two of the moves, RII and RIII (fig. A.1), involve only the crossings, and one more move, RI (A.3), involves the turning points as well. In addition, one should consider the transformations generated by the elementary transformations in fig. A.2, which involve only the turning points on the knot diagram [6].

### A.1.2 Topological invariance constraints on the crossing and turning point operators.

By definition, contraction (2.4) ignores the continuous, turning point-preserving planar transformations. Hence, the obtained quantity is a topological invariant provided that the operators  $\mathcal{R}$  and  $\mathcal{Q}$  satisfy a finite set of constraints explicitly presented below.


### A.2 Constraints on the $\mathcal{R}$ -matrices

Transformations in fig. A.1 are the planar projections of the continuous space transformations. Yet they affect non-trivially on the knot diagram and can be identified with the generators of the vertices changing subgroup of the entire equivalence transformations group. The corresponding space constraints on the vertex ( $\mathcal{R}$ ) operators are presented below each figure.

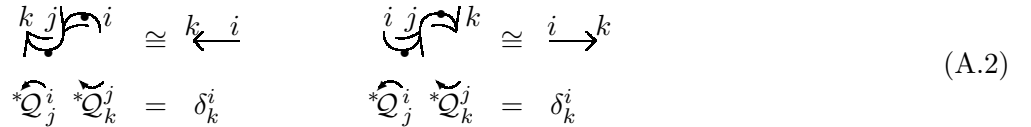


$$\begin{aligned}
 \begin{array}{c} k \quad l \\ \nearrow \quad \searrow \\ a \quad b \\ \nwarrow \quad \nearrow \\ i \quad j \end{array} &= \begin{array}{c} k \quad l \\ \curvearrowright \quad \curvearrowleft \\ i \quad j \end{array} \\
 {}^-\mathcal{R}_{ab}^{ji} {}^+\mathcal{R}_{kb}^{al} &= \delta_k^i \delta_l^j \\
 \begin{array}{c} k \quad l \\ \nearrow \quad \searrow \\ m \quad p \\ \nwarrow \quad \nearrow \\ c \quad a \\ i \quad j \end{array} &= \begin{array}{c} k \quad l \\ \nearrow \quad \searrow \\ m \quad p \\ \nwarrow \quad \nearrow \\ a \quad c \\ i \quad j \end{array} \\
 {}^*\mathcal{R}_{jc}^{ia} {}^*\mathcal{R}_{cm}^{pb} {}^*\mathcal{R}_{ak}^{bl} &= {}^*\mathcal{R}_{ia}^{pb} {}^*\mathcal{R}_{jc}^{bl} {}^*\mathcal{R}_{cm}^{ak}, \quad * \in \{+, -\}.
 \end{aligned} \tag{A.1}$$

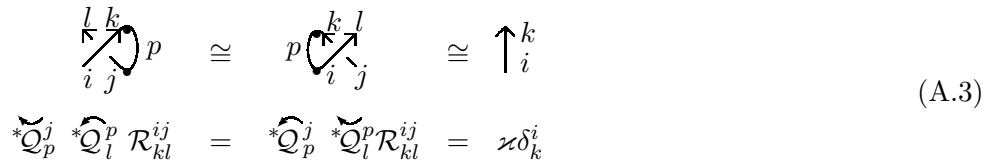
### A.3 Relations between the $\mathcal{R}$ and $\mathcal{Q}$ -matrices

**Extremum point operators.** The described approach to the knot invariants also requires for selecting a direction in the plane [34, 6, 35]. As a result, one must treat the turning points as two-valent vertices on the knot diagram of the four kinds, .

The equivalence transformations of the knot diagram that change the number of the turning points must be considered separately. These transformations form a finite subgroup, and their generators give rise to the relations between different  $\mathcal{Q}$ , as well as between  $\mathcal{R}$  and  $\mathcal{Q}$  matrices (both presented below).



$$\begin{aligned}
 \begin{array}{c} k \quad j \\ \nearrow \quad \searrow \\ i \end{array} &\cong \begin{array}{c} k \quad i \\ \leftarrow \end{array} & \begin{array}{c} i \quad j \\ \nwarrow \quad \nearrow \\ k \end{array} &\cong \begin{array}{c} i \quad k \\ \rightarrow \end{array} \\
 {}^*\check{\mathcal{Q}}_j^i {}^*\check{\mathcal{Q}}_k^j &= \delta_k^i & {}^*\check{\mathcal{Q}}_j^i {}^*\check{\mathcal{Q}}_k^j &= \delta_k^i
 \end{aligned} \tag{A.2}$$



$$\begin{aligned}
 \begin{array}{c} l \quad k \\ \nearrow \quad \searrow \\ i \quad j \\ p \end{array} &\cong \begin{array}{c} k \quad l \\ \nearrow \quad \searrow \\ i \quad j \\ p \end{array} &\cong \begin{array}{c} k \\ \uparrow \\ i \end{array} \\
 {}^*\check{\mathcal{Q}}_p^j {}^*\check{\mathcal{Q}}_l^p \mathcal{R}_{kl}^{ij} &= {}^*\check{\mathcal{Q}}_p^j {}^*\check{\mathcal{Q}}_l^p \mathcal{R}_{kl}^{ij} = \varkappa \delta_k^i
 \end{aligned} \tag{A.3}$$

The factor  $\varkappa$  here depends on the particular solutions of (A.1) for the  $\mathcal{R}$  operators. In particular,  $\varkappa = q^{-N}$  for solution (2.6).

**Framing factor.** Multiplied on  $\varkappa^w = q^{-wN}$ , where  $w \equiv \# \nearrow \searrow - \# \nwarrow \nearrow$  is the algebraic number of crossings on the knot diagram, contraction (2.4) becomes topologically invariant. One can set  $\varkappa = 1$  by using homogeneity property of constraints (A.1) to rescale the  $\mathcal{R} \rightarrow \varkappa \mathcal{R}$ . Yet the resulting  $\mathcal{R}$  explicitly depends on the chosen Lie algebra  $su_N$  via  $N$ , and this is why we do not make such rescaling here.

**Types of crossings in presence of the selected direction.** Once the preferred direction in the projection plane is chosen, one must consider 8 kinds of crossings instead of 2, 4 variants of each  $\nearrow$  and  $\nwarrow$ , differing by orientations of arrows w.r.t. the preferred direction. The topological invariance constraints then relate the corresponding 8 crossing operators to each other via the extremum point operators. The corresponding relations are given below.

$$\begin{array}{c}
 \begin{array}{ccc}
 \begin{array}{c} k \nearrow \\ l \nwarrow \\ i \end{array} & \cong & \begin{array}{c} \nearrow \\ \nwarrow \\ \end{array} \\
 \end{array} & \cong & \begin{array}{c} \nearrow \\ \nwarrow \\ \end{array} & \begin{array}{c} * \check{Q}_{j'}^j * \check{Q}_l^{i'} + \mathcal{R}_{k'l'}^{i'j'} \end{array} & (A.4)
 \end{array}$$

$$\begin{array}{c}
 \begin{array}{ccc}
 \begin{array}{c} i \nearrow \\ j \nwarrow \\ k \end{array} & \cong & \begin{array}{c} \nearrow \\ \nwarrow \\ \end{array} \\
 \end{array} & \cong & \begin{array}{c} \nearrow \\ \nwarrow \\ \end{array} & \begin{array}{c} * \check{Q}_{i'}^i * \check{Q}_k^{j'} + \mathcal{R}_{k'l'}^{i'j'} \end{array} & (A.5)
 \end{array}$$

$$\begin{array}{ccc}
 \begin{array}{c} +\mathcal{R}_{kl}^{ij} \\ \parallel \\ * \check{Q}_{j'}^j * \check{Q}_l^{i'} * \check{Q}_{i'}^i * \check{Q}_k^{j'} + \mathcal{R}_{k'l'}^{i'j'} \end{array} & \begin{array}{c} \begin{array}{c} l \nearrow \\ i \nwarrow \\ j \end{array} \\ \parallel \\ \begin{array}{c} j \nwarrow \\ k \nearrow \\ l \end{array} \end{array} & \begin{array}{c} -\mathcal{R}_{kl}^{ij} \\ \parallel \\ * \check{Q}_{i'}^i * \check{Q}_k^{j'} * \check{Q}_{j'}^j * \check{Q}_l^{i'} - \mathcal{R}_{k'l'}^{i'j'} \end{array} & \begin{array}{c} \begin{array}{c} k \nearrow \\ j \nwarrow \\ i \end{array} \\ \parallel \\ \begin{array}{c} i \nwarrow \\ l \nearrow \\ k \end{array} \end{array} & (A.6) \\
 \begin{array}{c} * \check{Q}_{j'}^j * \check{Q}_l^{i'} + \mathcal{R}_{k'l'}^{i'j'} \\ \parallel \\ * \check{Q}_{i'}^i * \check{Q}_k^{j'} + \mathcal{R}_{k'l'}^{i'j'} \end{array} & \begin{array}{c} \begin{array}{c} i \nwarrow \\ j \nearrow \\ k \end{array} \\ \parallel \\ \begin{array}{c} k \nearrow \\ l \nwarrow \\ i \end{array} \end{array} & \begin{array}{c} * \check{Q}_{i'}^i * \check{Q}_k^{j'} - \mathcal{R}_{k'l'}^{i'l} \\ \parallel \\ * \check{Q}_{k'}^k * \check{Q}_l^{i'} - \mathcal{R}_{k'l'}^{ij'} \end{array} & \begin{array}{c} \begin{array}{c} j \nearrow \\ i \nwarrow \\ l \end{array} \\ \parallel \\ \begin{array}{c} l \nearrow \\ k \nwarrow \\ j \end{array} \end{array}
 \end{array}$$

**The commutation relations.** Both  $\mathcal{R}$  operators must commute with the tensor squares of all the four  $\mathcal{Q}$  operators (we skip the corresponding equivalence transformations),

$$\check{Q}_{i'}^i \check{Q}_{j'}^j * \mathcal{R}_{kl}^{i'j'} = \check{Q}_k^{k'} \check{Q}_l^{l'} * \mathcal{R}_{k'l'}^{ij}, \quad * \in \{+, -\}, \quad \times \in \{ \curvearrowright, \curvearrowleft, \smile, \frown \}. \quad (A.7)$$

Relations (A.7) follow from relations (A.3, A.2) and provide the vertical equalities in relations (A.6).

**Freedom in the definition of the turning point operators.** Topological invariance constraints (A.3, A.2) fix only the pairwise products. Any four  $\mathcal{Q}$  operators satisfying equations (A.2, A.3) yield the same expression for the knot invariant [34, 6, 35]. In particular, one can select these operators as in (2.7), where the two operators are the unity operators, so that the related turning point can be ignored (just as we do through the text).

#### A.4 Properties of the particular solution

The  $+\mathcal{R}$ - and  $-\mathcal{R}$ -operators given by particular solution (2.6) of the topological invariance constraints also satisfy the *skein* relations, namely [33, 38]

$$\begin{array}{ccc}
 \begin{array}{c} l \nearrow \\ i \nearrow \\ j \end{array} \begin{array}{c} k \\ \nwarrow \\ i \end{array} - \begin{array}{c} k \nearrow \\ j \nearrow \\ i \end{array} \begin{array}{c} l \\ \nwarrow \\ i \end{array} & = & (q - q^{-1}) \begin{array}{c} k \\ \curvearrowright \\ i \end{array} \begin{array}{c} l \\ \curvearrowleft \\ j \end{array} \\
 +\mathcal{R}_{kl}^{ij} - \mathcal{R}_{kl}^{ij} & = & (q - q^{-1}) \delta_k^i \delta_l^j.
 \end{array} \quad (A.8)$$



These relations together with (A.1) lead to the characteristic equations

$$\left({}^+\mathcal{R} - q\right) \left({}^+\mathcal{R} + q^{-1}\right) = 0, \quad \left({}^-\mathcal{R} - q^{-1}\right) \left({}^-\mathcal{R} + q\right) = 0. \quad (\text{A.9})$$

Relations (A.9) imply that each of the crossing operators has just two distinct eigenvalues:  $q, (-q^{-1})$  for  ${}^+\mathcal{R}$ , and  $q^{-1}, (-q)$  for  ${}^-\mathcal{R}$ . The operators  $\mathcal{R}$  and  $\mathcal{Q}$  given by (2.6,2.7) (so that  $\mathcal{R}$  satisfies (A.9)) correspond to relating the space of fundamental representation of the  $\mathfrak{gl}_N$  algebra to each edge of the knot diagram. The choice of this space is essential for the entire construction, which in all versions [5, 4, 23, 3] heavily relies on decomposition (2.8), and hence on (A.9) whence the decomposition follows.

Although an analog of (2.8) is explicitly known for any representation of any simple Lie [38]), there are hardly any advances in extending the KhR construction beyond the fundamental representation of  $\mathfrak{gl}_N$ .

## A.5 Inverting of all crossings and mirror symmetry of the knot invariants

Many important knot invariants, among them are the Jones, HOMFLY, Khovanov, and the KhR invariants, possess the so called *mirror symmetry* [45]. The symmetry relates the expressions for the invariant for a knot and its mirror image. Generally these two knots are topologically distinct [6], and all the enumerated invariants do distinguish them. Still, the invariants for the knot and for its mirror image are related by simple change of the variables, e.g.,  $q \rightarrow 1/q, T \rightarrow 1/T$  for the KhR invariants.

The mirror transformation corresponds to inverting all the crossings  $\nearrow \leftrightarrow \nwarrow$  on the knot diagram. By this reason, only the diagrams with  $\# \nearrow > \# \nwarrow$  are usually considered. In particular, in case of two-strand braids it is enough to consider only  $\nearrow$  type crossings, just as we do in sec. 6.2.

## B The ‘‘graded’’ basis respected by the differentials

Here we describe in more details of the ‘‘graded’’ basis, selected in sec. 2.7 in the Khovanov complex and used in 2.8 to derive the Positive integer decomposition for the generating function  $\mathfrak{P}(q, T)$ .

Recall that by definition

$$\mathcal{V}_k = \text{Im } \hat{d}_k \oplus \text{coIm } \hat{d}_{k+1} \oplus H_k \Leftrightarrow x = \hat{d}_k y + z + h, \quad \forall x \in \mathcal{V}_k. \quad (\text{B.1})$$

In particular,  $x \in \text{coIm } \hat{d} \stackrel{\text{def}}{\Leftrightarrow} \hat{d}x \neq 0$ .

To simplify the subsequent formulas, we introduce the grading operator  $\hat{\Delta}$  such that  ${}^*\bar{\mathcal{Z}} = q^{\hat{\Delta}}$ . Then we chose the basis in the space  $\mathcal{V}_k$  composed of three groups of the vectors

$$\left\{ y_{k,i} : \hat{d}_{k+1} y_{k,i} \neq 0 \right\}_{i=1}^{\dim \text{Im } \hat{d}_{k+1}} \cup \left\{ z_{k,i} = \hat{d}_k y_{k-1,i} \right\}_{i=1}^{\dim \text{Im } \hat{d}_k} \cup \left\{ h_{k,i} \right\}_{i=1}^{\dim \mathcal{V}_k - \dim \text{Im } \hat{d}_k - \dim \text{Im } \hat{d}_{k+1}}, \quad (\text{B.2})$$

$$\hat{\Delta} y_{k,i} = \Delta_{k,i} y_{k,i} \quad \hat{\Delta} z_{k,i} = \Delta_{k-1,i} z_{k,i} \quad \hat{\Delta} h_{k,i} = \Delta'_{i,k} h_{k,i}$$

The groups are selected successively for all spaces  $\mathcal{V}_k$  ( $k = \overline{0, n}$ ) in the complex, and the transition  $k \rightarrow k+1$  is performed as follows. First, the vectors  $\left\{ z_{k,i} = \hat{d}_k y_{k-1,i} \right\}_{i=1}^{\dim \text{Im } \hat{d}_k}$  are linearly independent and graded by construction. Second, these vectors  $z$  span the space  $\text{Im } \hat{d}_k$ , which is an invariant subspace of the grading operator  $\hat{\Delta}$  (because  $x = \hat{d}_k y \Rightarrow \hat{\Delta} x = \hat{d}_k \Delta y \in \text{Im } \hat{d}$  for any  $y \in \hat{d}_k$ ). The factor space  $\text{coIm } \hat{d}_k \equiv \mathcal{V}_k / \text{Im } \hat{d}_k$ . Similarly, the factor space is also an invariant subspace of  $\hat{\Delta}$  and contains the graded basis

$$\{x_{k,i} \in \text{coIm}\}_{i=1}^{\dim \mathcal{V}_k - \dim \text{Im } \hat{d}_k}. \quad (\text{B.3})$$

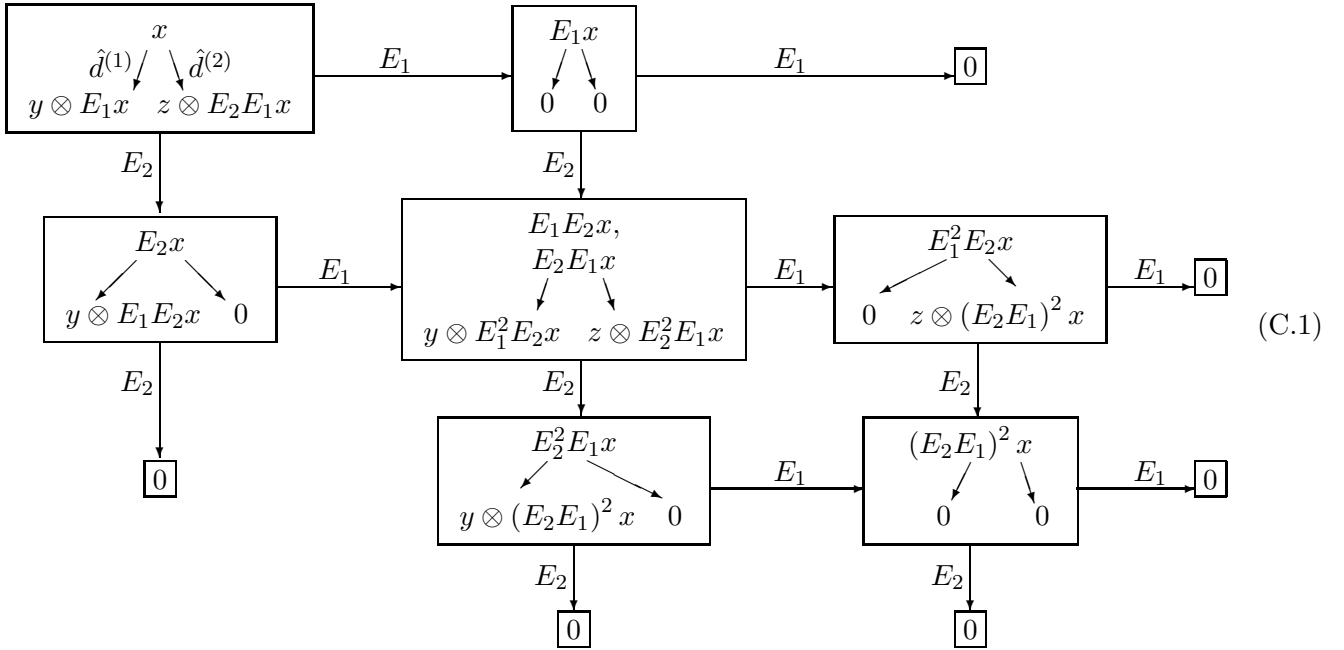
Next, the number of the linearly independent vectors among  $\{\hat{d}_{k+1}x_{i,k}\}_{i=1}^{\dim \mathcal{V}}$  is by definition  $\dim \text{Im } \hat{d}_{k+1}$ , and because  $\hat{d}_{k+1}z_{k,i} = 0$  for all  $i$  (due to the nilpotency condition  $\hat{d}_{k+1}\hat{d}_k = 0$ ), the basis vectors in  $\text{Im } \hat{d}_{k+1}$  must be among the vectors  $\hat{d}_{k+1}x_{k,i}$ .

Images of all the remaining basis vectors can be expanded as  $\hat{d}_{k+1}x_{k,j} = \sum_{i=1}^{\dim \text{Im } \hat{d}_{k+1}} \alpha_i \hat{d}_{k+1}y_{k,i}$  for some  $\alpha$  (in the particular case  $\hat{d}_{k+1}x_{k,l+1} = 0$  all  $\alpha = 0$ ). The vectors  $h_{k,i} \equiv x_{k,j} - \sum_{i=1}^{\dim \text{Im } \hat{d}_{k+1}} \alpha_i y_{k,i}$  form the basis in the homology space. Indeed, by definition  $\hat{d}_{k+1}h_{k,i} = 0$ , hence  $h_{k,i} \in \ker \hat{d}_{k+1}$ , and  $h_{k,i} \notin \text{Im } \hat{d}_k$ . These vectors are linearly independent thanks to the presence of  $x_{k,j}$ , and the number of them equals to the homology dimension.

The bases in  $\mathcal{V}_0$  and in  $\mathcal{V}_n$  can be chosen just in same way, if we assume that  $\mathcal{V}_{-1} \equiv \emptyset$  and  $\mathcal{V}_{n+1} \equiv \emptyset$ , respectively.

## C Morphisms of the representation spaces. A more involved example

Here we provide one more illustration of the representation theory standpoint on the KhR formalism discussed in sec. 4. The figure below demonstrates a non-trivial (not exact) map between two  $[2, 1]$  representations of the  $su_3$  algebra [38]. This map has the same properties as the morphisms in sec. 4.



## D List of braids providing the unique level I reminders

The first-level minimal positive integer division of the primary polynomial, the type	
Uniquely determined	Ambiguous
$0_1 \cup 0_1$ , the pair of unlinked Unknots	
[1], [2].	
$0_1$ , the Unknot, Torus [2, 1]	
[21], [12].	
$0_1 \cup 2_1^1$ , the Hopf link unlinked with the Unknot	
[22], [11].	
$2_1^1$ , the Hopf link, Torus [2, 2]	
[221], [122], [121], [112], [211], [212].	
$0_1 \cup 3_1$ , the Trefoil knot as Torus [2, 3] unlinked with the Unknot	
[222], [111].	
$3_1$ , the Trefoil knot, as Torus [3, 2]	
[1211], [2221], [2122], [1222], [1112], [1212], [2121], [2212], [2111], [1121].	
$4_1^2$ , $L4a1(1)$ , the Solomon link, Torus [2, 4]	
[22122], [21222], [21211], [22121], [12111], [12112], [11212], [12122], [11121], [22212], [21221], [12212], [11211], [22221], [21111], [12222], [11112].	
[21221], [12212], [11211], [21212], [12121], [21121].	
$5_1$ , the Fivefoil knot, Torus [2, 5]	
[121122], [121211], [222212], [212111], [212122], [121111], [111212], [222122], [122121], [212222], [211212], [212211], [212112], [112122], [121112], [122112], [212221], [121221], [221222], [122212], [112121], [211221], [121222], [221121], [111211], [221212], [222121], [211121], [112212], [111121], [221211], [112111].	[222221], [122222], [111112], [211111].
$6_3^3$ , $L6n1(0, 1)$ , Torus [3, 3]	
[211211], [221221], [121121], [121212], [212121], [122122], [212212], [112112].	
$7_7^2$ , $L7n1(0)$	
[1221212], [1221221], [1211121], [2122121], [1121112], [2211221], [2121221], [1212112], [1112112], [2121121], [2122122], [1222122], [1221222], [2121212], [1121212], [2112111], [2212221], [2121211], [2112121], [2111211], [2122212], [1122112], [2112112], [1212122], [1221122], [2112211], [1212121], [1212212], [2212121], [2221221], [1211212], [2212212], [1121121], [121121].	[2211211], [1121122], [2212211], [1221121], [1122122], [1211221], [2112212], [2122112].
$8_{19}$ , Torus [3, 4], the first "thick" knot	
[12212212], [21211211], [11121122], [21221221], [22122121], [22212211], [21121211], [21121121], [11221222], [12112112], [21212121], [11212122], [12122122], [12212122], [22112111], [22121211], [11212112], [11211212], [22121221], [12121212].	[12112211], [21221122], [22211221], [12211212], [11221112], [11211121], [12112121], [21121112], [12121121], [22112221], [22122212], [11222122], [21122111], [21122212], [12121122], [12111221], [22112121], [21121221], [21112112], [21112211], [12212222], [11221121], [21212211], [21221212], [11211221], [22212221], [11211122], [11122112], [22122112], [12221122], [21122121], [12212121], [12212221], [21121212], [12112212], [22111211], [11221212], [22112212], [12211211], [21221121], [21221122].

# E Examples of the unique minimal remainders related to the CohFT diagrams in the case of three strands

## E.1 The doubly twisted diagram of the unknot

[1, 2], the doubly twisted unknot				
$T$ -grading	$q$ -grading	$\chi$	Diagrams	Khovanov polynomial, $q$ -gradings of the terms
0	$2 + \Delta_{111}$	1		3, 1
	$2 + \Delta_{001}$	1		
	$2 + \Delta_{011}$	1		
	$2 + \Delta_{000}$	1		
1	$\Delta_{011}$	-1		
	$\Delta_{001}$	-1		

(E.1)

## E.2 The trefoil knot in different three strand presentations

1. [1112], the Trefoil knot				
$T$ -grading	$q$ -grading	$ \chi $	Diagrams	Khovanov polynomial, $q$ -gradings of the terms
0	$4 + \Delta_{111}$	1		-1, -3
	$4 + \Delta_{000}$	1		
	$4 + \Delta_{001}$	1		
	$4 + \Delta_{011}$	1		
1	$2 + \Delta_{011}$	1		
	$2 + \Delta_{001}$	1		
2	$2 + \Delta_{100}$	1		-5
	$2 + \Delta_{101}$	1		
	$\Delta_{011}$	1		
3	$2 + \Delta_{011}$	1		-9
	$\Delta_{101}$	2		
	$\Delta_{100}$	1		
4	$2 + \Delta_{101}$	1		

2. [1121], the Trefoil knot				
$T$ -grading	$q$ -grading	$ \chi $	Diagrams	Khovanov polynomial, $q$ -gradings of the terms
0	$4 + \Delta_{111}$	1		-1, -3
	$4 + \Delta_{000}$	1		
	$4 + \Delta_{011}$	1		
	$4 + \Delta_{001}$	1		
1	$2 + \Delta_{001}$	1		
	$2 + \Delta_{011}$	1		
2	$2 + \Delta_{101}$	1		-5
	$2 + \Delta_{010}$	1		
3	$\Delta_{101}$	1		-9
	$\Delta_{010}$	1		

3. [1211], the Trefoil knot				
$T$ -grading	$q$ -grading	$ \chi $	Diagrams	Khovanov polynomial, $q$ -gradings of the terms
0	$4 + \Delta_{001}$	1	$\begin{bmatrix}   &   &   \\ \uparrow \end{bmatrix}$	-1, -3
	$4 + \Delta_{011}$	1	$\begin{bmatrix} \uparrow & \uparrow & \uparrow \\   \end{bmatrix}$	
	$4 + \Delta_{111}$	1	$\begin{bmatrix}   &   &   \\   \end{bmatrix}$	
	$4 + \Delta_{000}$	1	$\begin{bmatrix}   &   &   \\   \end{bmatrix}$	
1	$2 + \Delta_{001}$	1	$\begin{bmatrix}   &   &   \\ \uparrow \bullet \end{bmatrix}$	
	$2 + \Delta_{011}$	1	$\begin{bmatrix} \uparrow \bullet & \uparrow \uparrow \\   \end{bmatrix}, \begin{bmatrix} \uparrow & \uparrow \bullet \uparrow \\   \end{bmatrix}, \begin{bmatrix} \uparrow & \uparrow \uparrow \bullet \\   \end{bmatrix}$	
2	$2 + \Delta_{101}$	1	$\begin{bmatrix} \times & \uparrow & \times \\   \end{bmatrix}$	-5
	$2 + \Delta_{010}$	1	$\begin{bmatrix} \times & \times & \uparrow \\   \end{bmatrix}$	
3	$\Delta_{010}$	1	$\begin{bmatrix} \times & \times & \uparrow \bullet \\   \end{bmatrix}$	-9
	$\Delta_{101}$	1	$\begin{bmatrix} \times & \uparrow \bullet & \times \\   \end{bmatrix}$	

4. [2111], the Trefoil knot				
$T$ -grading	$q$ -grading	$ \chi $	Diagrams	Khovanov polynomial, $q$ -gradings of the terms
0	$4 + \Delta_{111}$	1	$\begin{bmatrix}   &   &   \\   \end{bmatrix}$	-1, -3
	$4 + \Delta_{000}$	1	$\begin{bmatrix}   &   &   \\   \end{bmatrix}$	
	$4 + \Delta_{011}$	1	$\begin{bmatrix} \uparrow & \uparrow & \uparrow \\   \end{bmatrix}$	
	$4 + \Delta_{001}$	1	$\begin{bmatrix}   &   &   \\ \uparrow \end{bmatrix}$	
1	$2 + \Delta_{001}$	1	$\begin{bmatrix}   &   &   \\ \uparrow \bullet \end{bmatrix}$	
	$2 + \Delta_{011}$	1	$\begin{bmatrix} \uparrow \bullet & \uparrow \uparrow \\   \end{bmatrix}, \begin{bmatrix} \uparrow & \uparrow \bullet \uparrow \\   \end{bmatrix}, \begin{bmatrix} \uparrow & \uparrow \uparrow \bullet \\   \end{bmatrix}$	
2	$2 + \Delta_{101}$	1	$\begin{bmatrix} \times & \uparrow & \times \\ \uparrow \end{bmatrix}$	-5
	$\Delta_{011}$	1	$\begin{bmatrix} \uparrow \bullet & \uparrow \bullet \uparrow \\   \end{bmatrix}, \begin{bmatrix} \uparrow \bullet & \uparrow \uparrow \bullet \\   \end{bmatrix}, \begin{bmatrix} \uparrow & \uparrow \bullet \uparrow \bullet \\   \end{bmatrix}$	
	$2 + \Delta_{100}$	1	$\begin{bmatrix} \times & \uparrow & \times \\   \end{bmatrix}$	
3	$\Delta_{100}$	1	$\begin{bmatrix} \times & \uparrow \bullet & \times \\   \end{bmatrix}$	-9
	$\Delta_{101}$	2	$\begin{bmatrix} \times & \uparrow & \times \\ \uparrow \bullet \end{bmatrix}, \begin{bmatrix} \times & \uparrow \bullet & \times \\ \uparrow \end{bmatrix}$	
	$2 + \Delta_{011}$	1	$\begin{bmatrix} \uparrow \bullet & \uparrow \bullet \uparrow \\   \end{bmatrix}$	
4	$2 + \Delta_{101}$	1	$\begin{bmatrix} \times & \uparrow \bullet & \times \\ \uparrow \bullet \end{bmatrix}$	

5. [1222], the Trefoil knot

$T$ -grading	$q$ -grading	$ \chi $	Diagrams	Khovanov polynomial, $q$ -gradings of the terms
0	$4 + \Delta_{001}$	1	$\left[ \begin{array}{c}   \\ \uparrow \uparrow \uparrow \end{array} \right]$	-1, -3
	$4 + \Delta_{011}$	1	$\left[ \begin{array}{c} \uparrow \\   \\   \\   \end{array} \right]$	
	$4 + \Delta_{111}$	1	$\left[ \begin{array}{c}   \\   \\   \\   \end{array} \right]$	
	$4 + \Delta_{000}$	1	$\left[ \begin{array}{c}   \\   \\   \\   \end{array} \right]$	
1	$2 + \Delta_{001}$	1	$\left[ \begin{array}{c}   \\ \uparrow \uparrow \uparrow \\ \bullet \uparrow \uparrow \end{array} \right], \left[ \begin{array}{c}   \\ \uparrow \uparrow \uparrow \\ \uparrow \bullet \uparrow \end{array} \right], \left[ \begin{array}{c}   \\ \uparrow \uparrow \uparrow \\ \uparrow \uparrow \bullet \end{array} \right]$	
	$2 + \Delta_{011}$	1	$\left[ \begin{array}{c} \uparrow \\   \\   \\   \\ \bullet \end{array} \right]$	
2	$2 + \Delta_{110}$	1	$\left[ \begin{array}{c}   \\ \times \uparrow \times \end{array} \right]$	-5
	$\Delta_{001}$	1	$\left[ \begin{array}{c}   \\ \uparrow \uparrow \uparrow \\ \bullet \uparrow \uparrow \end{array} \right], \left[ \begin{array}{c}   \\ \uparrow \uparrow \uparrow \\ \uparrow \bullet \uparrow \end{array} \right], \left[ \begin{array}{c}   \\ \uparrow \uparrow \uparrow \\ \uparrow \uparrow \bullet \end{array} \right]$	
	$2 + \Delta_{010}$	1	$\left[ \begin{array}{c} \uparrow \\   \\ \times \uparrow \times \end{array} \right]$	
3	$\Delta_{110}$	1	$\left[ \begin{array}{c}   \\ \times \uparrow \times \\ \bullet \end{array} \right]$	-9
	$\Delta_{010}$	2	$\left[ \begin{array}{c} \uparrow \\   \\ \times \uparrow \times \\ \bullet \end{array} \right], \left[ \begin{array}{c} \uparrow \\   \\ \times \uparrow \times \\ \bullet \end{array} \right]$	
	$2 + \Delta_{001}$	1	$\left[ \begin{array}{c}   \\ \uparrow \uparrow \uparrow \\ \bullet \uparrow \uparrow \end{array} \right]$	
4	$2 + \Delta_{010}$	1	$\left[ \begin{array}{c} \uparrow \\   \\ \times \uparrow \times \\ \bullet \end{array} \right]$	

6. [2122], the Trefoil knot

$T$ -grading	$q$ -grading	$ \chi $	Diagrams	Khovanov polynomial, $q$ -gradings of the terms
0	$4 + \Delta_{111}$	1	$\left[ \begin{array}{c}   \\   \\   \\   \end{array} \right]$	-1, -3
	$4 + \Delta_{000}$	1	$\left[ \begin{array}{c}   \\   \\   \\   \end{array} \right]$	
	$4 + \Delta_{011}$	1	$\left[ \begin{array}{c} \uparrow \\   \\   \\   \end{array} \right]$	
	$4 + \Delta_{001}$	1	$\left[ \begin{array}{c}   \\ \uparrow \uparrow \uparrow \end{array} \right]$	
1	$2 + \Delta_{001}$	1	$\left[ \begin{array}{c}   \\ \uparrow \uparrow \uparrow \\ \bullet \uparrow \uparrow \end{array} \right], \left[ \begin{array}{c}   \\ \uparrow \uparrow \uparrow \\ \uparrow \bullet \uparrow \end{array} \right], \left[ \begin{array}{c}   \\ \uparrow \uparrow \uparrow \\ \uparrow \uparrow \bullet \end{array} \right]$	
	$2 + \Delta_{011}$	1	$\left[ \begin{array}{c} \uparrow \\   \\   \\   \\ \bullet \end{array} \right]$	
2	$2 + \Delta_{101}$	1	$\left[ \begin{array}{c}   \\ \times \times \uparrow \end{array} \right]$	-5
	$2 + \Delta_{010}$	1	$\left[ \begin{array}{c}   \\ \times \uparrow \times \end{array} \right]$	
3	$\Delta_{101}$	1	$\left[ \begin{array}{c}   \\ \times \times \uparrow \\ \bullet \end{array} \right]$	-9
	$\Delta_{010}$	1	$\left[ \begin{array}{c}   \\ \times \uparrow \times \\ \bullet \end{array} \right]$	

7. [2212], the Trefoil knot				
$T$ -grading	$q$ -grading	$ \chi $	Diagrams	Khovanov polynomial, $q$ -gradings of the terms
0	$4 + \Delta_{001}$	1	$\begin{bmatrix}   \\ \uparrow \uparrow \uparrow \end{bmatrix}$	-1, -3
	$4 + \Delta_{011}$	1	$\begin{bmatrix} \uparrow \\       \end{bmatrix}$	
	$4 + \Delta_{111}$	1	$\begin{bmatrix}   \\       \end{bmatrix}$	
	$4 + \Delta_{000}$	1	$\begin{bmatrix}   \\       \end{bmatrix}$	
1	$2 + \Delta_{001}$	1	$\begin{bmatrix}   \\ \uparrow \uparrow \uparrow \end{bmatrix}, \begin{bmatrix}   \\ \uparrow \uparrow \uparrow \end{bmatrix}, \begin{bmatrix}   \\ \uparrow \uparrow \uparrow \end{bmatrix}$	
	$2 + \Delta_{011}$	1	$\begin{bmatrix} \uparrow \\       \end{bmatrix}$	
2	$2 + \Delta_{101}$	1	$\begin{bmatrix}   \\ \uparrow \times \times \end{bmatrix}$	-5
	$2 + \Delta_{010}$	1	$\begin{bmatrix}   \\ \times \uparrow \times \end{bmatrix}$	
3	$\Delta_{010}$	1	$\begin{bmatrix}   \\ \times \uparrow \times \end{bmatrix}$	-9
	$\Delta_{101}$	1	$\begin{bmatrix}   \\ \uparrow \times \times \end{bmatrix}$	

8. [2221], the Trefoil knot				
$T$ -grading	$q$ -grading	$ \chi $	Diagrams	Khovanov polynomial, $q$ -gradings of the terms
0	$4 + \Delta_{111}$	1	$\begin{bmatrix}   \\       \end{bmatrix}$	-1, -3
	$4 + \Delta_{000}$	1	$\begin{bmatrix}   \\       \end{bmatrix}$	
	$4 + \Delta_{011}$	1	$\begin{bmatrix} \uparrow \\       \end{bmatrix}$	
	$4 + \Delta_{001}$	1	$\begin{bmatrix}   \\ \uparrow \uparrow \uparrow \end{bmatrix}$	
1	$2 + \Delta_{001}$	1	$\begin{bmatrix}   \\ \uparrow \uparrow \uparrow \end{bmatrix}, \begin{bmatrix}   \\ \uparrow \uparrow \uparrow \end{bmatrix}, \begin{bmatrix}   \\ \uparrow \uparrow \uparrow \end{bmatrix}$	
	$2 + \Delta_{011}$	1	$\begin{bmatrix} \uparrow \\       \end{bmatrix}$	
2	$2 + \Delta_{110}$	1	$\begin{bmatrix}   \\ \times \uparrow \times \end{bmatrix}$	-5
	$2 + \Delta_{010}$	1	$\begin{bmatrix} \uparrow \\ \times \uparrow \times \end{bmatrix}$	
	$\Delta_{001}$	1	$\begin{bmatrix}   \\ \uparrow \uparrow \uparrow \end{bmatrix}, \begin{bmatrix}   \\ \uparrow \uparrow \uparrow \end{bmatrix}, \begin{bmatrix}   \\ \uparrow \uparrow \uparrow \end{bmatrix}$	
3	$\Delta_{110}$	1	$\begin{bmatrix}   \\ \times \uparrow \times \end{bmatrix}$	-9
	$\Delta_{010}$	2	$\begin{bmatrix} \uparrow \\ \times \uparrow \times \end{bmatrix}, \begin{bmatrix} \uparrow \\ \times \uparrow \times \end{bmatrix}$	
	$2 + \Delta_{001}$	1	$\begin{bmatrix}   \\ \uparrow \uparrow \uparrow \end{bmatrix}$	
4	$2 + \Delta_{010}$	1	$\begin{bmatrix}   \\ \times \uparrow \times \end{bmatrix}$	



9. [1212]., the Trefoil knot					10. [2121], the Trefoil knot				
$T$ -grading	$q$ -grading	$ \chi $	Diagrams	Khovanov polynomial, $q$ -gradings of the terms	$T$ -grading	$q$ -grading	$ \chi $	Diagrams	Khovanov polynomial, $q$ -gradings of the terms
0	$4 + \Delta_{111}$	1	$\begin{bmatrix}   &   \\   &   \end{bmatrix}$	-1, -3	0	$4 + \Delta_{001}$	1	$\begin{bmatrix}   &   \\ \uparrow & \uparrow \end{bmatrix}$	-1, -3
	$4 + \Delta_{000}$	1	$\begin{bmatrix}   &   \\   &   \end{bmatrix}$			$4 + \Delta_{011}$	1	$\begin{bmatrix} \uparrow & \uparrow \\   &   \end{bmatrix}$	
	$4 + \Delta_{011}$	1	$\begin{bmatrix} \uparrow & \uparrow \\   &   \end{bmatrix}$			$4 + \Delta_{111}$	1	$\begin{bmatrix}   &   \\   &   \end{bmatrix}$	
	$4 + \Delta_{001}$	1	$\begin{bmatrix}   &   \\ \uparrow & \uparrow \end{bmatrix}$			$4 + \Delta_{000}$	1	$\begin{bmatrix}   &   \\   &   \end{bmatrix}$	
1	$2 + \Delta_{001}$	1	$\begin{bmatrix}   &   \\ \uparrow & \uparrow \end{bmatrix}, \begin{bmatrix}   &   \\ \uparrow & \uparrow \end{bmatrix}$		1	$2 + \Delta_{001}$	1	$\begin{bmatrix}   &   \\ \uparrow & \uparrow \end{bmatrix}, \begin{bmatrix}   &   \\ \uparrow & \uparrow \end{bmatrix}$	
	$2 + \Delta_{011}$	1	$\begin{bmatrix} \uparrow & \uparrow \\   &   \end{bmatrix}, \begin{bmatrix} \uparrow & \uparrow \\   &   \end{bmatrix}$			$2 + \Delta_{011}$	1	$\begin{bmatrix} \uparrow & \uparrow \\   &   \end{bmatrix}, \begin{bmatrix} \uparrow & \uparrow \\   &   \end{bmatrix}$	
2	$2 + \Delta_{101}$	1	$\begin{bmatrix} \times & \times \\   & \uparrow \end{bmatrix}$	-5	2	$2 + \Delta_{101}$	1	$\begin{bmatrix} \times & \times \\ \uparrow &   \end{bmatrix}$	-5
	$2 + \Delta_{010}$	1	$\begin{bmatrix} \uparrow &   \\ \times & \times \end{bmatrix}$			$2 + \Delta_{010}$	1	$\begin{bmatrix}   & \uparrow \\ \times & \times \end{bmatrix}$	
3	$\Delta_{101}$	1	$\begin{bmatrix} \times & \times \\   & \uparrow \end{bmatrix}$	-9	3	$\Delta_{010}$	1	$\begin{bmatrix}   & \uparrow \\ \times & \times \end{bmatrix}$	-9
	$\Delta_{010}$	1	$\begin{bmatrix} \uparrow &   \\ \times & \times \end{bmatrix}$			$\Delta_{101}$	1	$\begin{bmatrix} \times & \times \\ \uparrow &   \end{bmatrix}$	

